



# Trace metals in coastal marine sediments: Natural and anthropogenic sources, correlation matrices, and proxy potentials

K. Mareike Paul<sup>a,\*</sup>, Niels A.G.M. van Helmond<sup>b,c</sup>, Caroline P. Slomp<sup>b,c</sup>, Tom Jilbert<sup>a</sup>

<sup>a</sup> Environmental Geochemistry Group, Department of Geography and Geosciences, Faculty of Science, University of Helsinki, Helsinki, P.O 64 (Gustaf Hällströmin katu 2), FI-00014, Finland

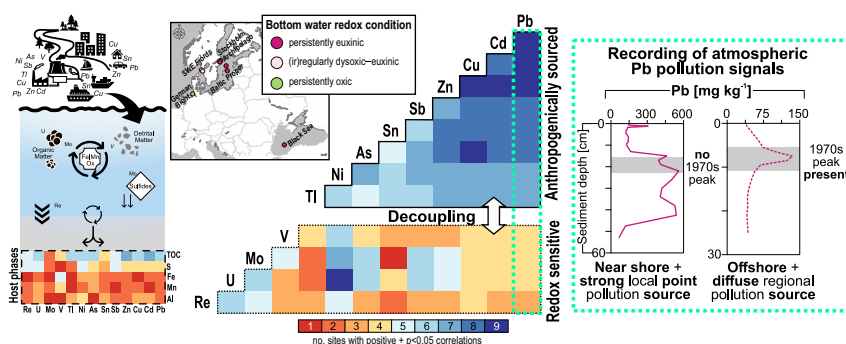
<sup>b</sup> Department of Earth Sciences, Faculty of Geosciences, Utrecht University, Utrecht 3584 CB, the Netherlands

<sup>c</sup> Radboud Institute for Biological and Environmental Sciences, Faculty of Science, Radboud University, Nijmegen 6525 AJ, the Netherlands

## HIGHLIGHTS

- Controls of trace metal deposition in human-impacted coastal sediments were studied.
- Combining correlations from multiple sites allows identification of common patterns.
- Positive correlations of Pb, Zn and Sn are primarily caused by common pollution sources.
- Cadmium, Zn, Cu and Sb are also markedly influenced by changes in oxygen concentrations.
- Lead most robustly records pollution as a function of distance from shore and source.

## GRAPHICAL ABSTRACT



## ARTICLE INFO

Editor: Julian Blasco

### Keywords:

Trace element covariation  
Redox-sensitive  
Near-shore depositional environment  
Metal pollution  
Deoxygenation  
R corplot

## ABSTRACT

Rapidly spreading industrialization since the 19th century has led to a drastic increase in trace metal deposition in coastal sediments. Provided that these trace metals have remained relatively immobile after deposition, their sedimentary enrichments can serve as records of local–regional pollution histories. Factors controlling this proxy potential include trace metal geochemistry (carrier-, and host phase affinity), and depositional environmental factors (redox variability, particulate shuttling, organic matter loading, bathymetry). Yet, the relative importance and interactions between these controls are still poorly understood, hampering the reliable use of trace metal-based environmental proxies. By summarizing nine site-specific correlation matrices of 16 metal (loid)s (Pb, Cd, Cu, Zn, Sb, Sn, Ni, As, Tl, V, Mo, U, Re, Fe, Mn, Al), total organic C, and S contents in short sediment cores into a single meta-matrix, we test a novel approach for quickly detecting common and contrasting trace metal enrichment patterns across different study locations. Our meta-matrix shows two trace metal groups, within which positive correlations of e.g., Pb, Cd, Zn, Cu, Sb suggest a primary “anthropogenically sourced” (group I) control, whereas known “redox-sensitive” (group II) trace metals (Mo, U, Re) are characterized by fewer positive correlations. However, some group I metals (Cd, Zn, Cu, Sb) also covary with group II metals, inferring that redox variability may obscure primary anthropogenic signals; Sb even shows advantages over Mo and U under oxic conditions. As a more robust pollution indicator we identified Pb; yet for reconstructing historical Pb atmospheric pollution signals (1970s Pb peak), it is crucial to consider the distance from shore. In near-shore

\* Corresponding author.

E-mail address: [mareike.paul@helsinki.fi](mailto:mareike.paul@helsinki.fi) (K.M. Paul).

<https://doi.org/10.1016/j.scitotenv.2024.175789>

Received 22 April 2024; Received in revised form 2 August 2024; Accepted 23 August 2024

Available online 26 August 2024

0048-9697/© 2024 The Authors. Published by Elsevier B.V. This is an open access article under the CC BY license (<http://creativecommons.org/licenses/by/4.0/>).

environments, local (fluvial) pollution signals may overprint large-scale (atmospheric) signals. Our findings demonstrate that combining site-specific sedimentary correlation and distribution patterns with a meta-matrix considerably aids the understanding of trace metal sequestration in different coastal sedimentary environments, which thereby improves trace metal proxy reliability.

## 1. Introduction

The accumulation of anthropogenically sourced trace metals and metalloids in coastal marine areas is a pressing social-environmental concern (OSPAR, 2017; HELCOM, 2018; EEA, 2019). While many trace metals naturally occur in the coastal environment, excess inputs from human activities can lead to concentrations above which they can become toxic to the surrounding ecosystem (e.g., Callender, 2014). Anthropogenic trace metals can enter the coastal environment as airborne particulates (via dry or wet atmospheric deposition), which can be transported from distal terrestrial sources and spread over large distances as far as several thousands of kilometers (e.g., Goldberg et al., 1981; Hallberg, 1991; Renberg et al., 2000) or as waterborne dissolved or particulate phases (via rivers/estuaries, groundwater, or coastal runoff), which often derive from local point sources (e.g., Nriagu and Pacyna, 1988; Callender, 2014). Key sources of anthropogenic trace metals are industry (mining and smelting), energy production (fossil fuel combustion), manufacturing (batteries, iron, and steel), agriculture (fertilizer use), transportation (petrol and tire wear), and urban activities (wastewater incineration) (Nriagu and Pacyna, 1988; Callender, 2014; OSPAR, 2017; EEA, 2019; HELCOM, 2021).

Historically, the earliest records of anthropogenic metal pollution date back to the Roman and Medieval periods (Murozumi et al., 1969; Brännvall et al., 1999; Renberg et al., 2001a; Cooke and Bindler, 2015). However, the strongest and most rapid rise in trace metal contents in many European lake and coastal marine sediments is generally linked to industrial expansion in the 19th and 20th centuries (e.g., Brännvall et al., 1999; Renberg et al., 2001a; van Helmond et al., 2020b). Particularly the combustion of fossil-fuel, including leaded gasoline can be tracked by peak Pb (and other metal) contents around the mid-20th century (Chow et al., 1973; Valette-Silver, 1993; Renberg et al., 2001a). Stricter emission controls and policies (e.g., the ban of leaded gasoline in 2000 in Europe; Larsen et al., 2012) have led to a gradual decrease in trace metal emissions since mid-20th century, particularly since the 1990s (OSPAR, 2017; HELCOM, 2018; EEA, 2019). While this emission decrease is also reflected in declining trace metal contents in coastal sediments, they still exceed natural background concentrations in many coastal regions (OSPAR, 2017; HELCOM, 2018; EEA, 2019). These legacy trace metal enrichments are the result of complex interactions between two types of factors influencing the fate of trace metals in coastal sediments. The first type includes the geochemical characteristics of a trace metal, such as the speciation and affinity for carrier phases – iron (Fe) and manganese (Mn) (oxy)(hydr)oxides (Fe and Mn oxides), aluminosilicates (clays), organic matter (OM), carbonates, and sulfides – particle-reactivity, and redox-stability (e.g., Tribouvillard et al., 2006; Bruland et al., 2014; Dang et al., 2015). The second one comprises the properties of, and geochemical-, biological-, and physical processes within a depositional environment (e.g., redox variability, particulate shuttling, organic matter loading, bathymetry), including those occurring *post* deposition (diagenesis, Calmano et al., 1993; Du Laing et al., 2007; Outridge and Wang, 2015).

The combined effect of these two types of factors controls the extent to which a trace metal is permanently buried in the sediment or prone to remobilization and lost from the sediment. For example, under suboxic (oxygen,  $O_2 = 0\text{--}0.2 \text{ mL L}^{-1}$ ), and particularly euxinic (total hydrogen sulfide,  $O_2 = 0$  and  $\sum H_2S > 0 \text{ mL L}^{-1}$ ) conditions, trace metals are generally more efficiently removed from the water column and pore waters, either by precipitating as or co-precipitating with relatively refractory mineral phases, such as carbonates, sulfides or sulfurized OM

(Hallberg, 1976; Outridge and Wang, 2015). As long as reducing conditions remain relatively stable, sediments can act as permanent sinks for anthropogenic trace metals (Rigaud et al., 2013; Bruland et al., 2014). However, post-depositional processes, such as inflow events of oxygenated water masses, and vertical or lateral reworking of surface sediments (e.g., by bioturbation, wave action, currents, dredging) can result in changing bottom water and sedimentary redox conditions, which may trigger re-suspension and -mobilization of formerly buried trace metals (Förstner et al., 1986; Calmano et al., 1993; Outridge and Wang, 2015). Depending on the element- and site-specific geochemical conditions, the dissolved trace metals may either re-(co)precipitate (with other mineral phases) vertically offset from the original sequestration depth, or diffuse back into the water column as a dissolved species, thereby turning sediments into a source (Salomons et al., 1987; Du Laing et al., 2009; Rigaud et al., 2013; Bruland et al., 2014; Dang et al., 2015). Both processes can alter the trace metal signal initially recorded in the sediment to such an extent that the reliability of trace metals as indicators of past environmental change and pollution history is significantly weakened or lost entirely (e.g., Outridge and Wang, 2015).

Many studies of trace metals in coastal sediments focus on the sources and/or accumulation of trace metals on a local to regional scale (Irion, 1994; Beck et al., 2013; Jokinen et al., 2020a), investigate a narrow selection of elements – mostly lead (Pb), zinc (Zn), and cadmium (Cd; Irion, 1994; Boxberg et al., 2020) due to both their strong and widespread enrichments as a consequence of extensive (pre)industrial use and toxicity for marine life and humans (Pb, Cd; OSPAR, 2017; HELCOM, 2021) –, or attempt to quantify trace metal contamination in the surface sediments (Kersten et al., 1988; Borg and Jonsson, 1996; Beck et al., 2013; Vallius et al., 2022). Several studies have investigated the geochemical behavior and host phases of different trace metals in coastal sediments considering whole sediment cores (Scholz and Neumann, 2007; Dang et al., 2015; van Helmond et al., 2018; Jokinen et al., 2020a), and have explored the impact of salinity, pH, dissolved organic C, and redox variability on trace metal mobility in coastal and estuarine/river sediments (Förstner et al., 1990; Gambrell et al., 1991; Rosenthal et al., 1995; Guo et al., 1997; Nameroff et al., 2002; Canuto et al., 2013; Luo et al., 2022). However, a systematic comparison of anthropogenically sourced trace metal behavior and enrichment pathways for different coastal depositional environments is still lacking. This has implications e.g., for interpreting trace metal contaminations in coastal sediments as a function of past and ongoing anthropogenic pollution.

Here, we aim to improve the understanding of trace metal behavior, covariation patterns and enrichment pathways in coastal marine sediments. Considering 13 trace metals – Pb, Cd, copper (Cu), Zn, antimony (Sb), tin (Sn), nickel (Ni), arsenic (As), thallium (Tl), vanadium (V), molybdenum (Mo), uranium (U), and rhenium (Re) – and nine contrasting coastal marine depositional environments (oxic–sulfidic, unrestricted–semi-enclosed, brackish–marine, near coastal–distant, shallow–deep), which cover the trace metal accumulation over the last century, we study co-enrichment patterns among elements to (1) investigate the importance of depositional and post-depositional factors in controlling anthropogenic trace metal distribution, (2) discuss potentials and limitations when applying sedimentary trace metals as chronological archives of anthropogenic pollution in coastal environments, and (3) assess the redox proxy potential of other trace metals alongside the most widely and best understood trace metal redox proxies, Mo and U.

## 2. Materials and methods

### 2.1. Selection of sites, elements, and data filtering

In our analysis we use sedimentary trace metal data from nine coastal marine sites (Fig. 1). These sites were selected because they cover a wide range of different depositional environmental characteristics, such as bottom water and sediment redox conditions, bathymetry, sedimentation rate, eutrophication, OM input, salinity, and their local and regional metal pollution history (Fig. 1 and Table 1). Crucial for the selection was further that the study sites are relatively well-understood with respect to above characteristics (van Helmond et al., 2018, 2020b; Jokinen et al., 2020a, 2020b; Paul et al., 2023a) to provide a comprehensive understanding of trace metal dynamics as a function of different depositional environmental factors. For our investigation of the impact of redox conditions/variability on the trace metals, the study sites were grouped based on the average modern bottom water redox conditions at each location (Paul et al., 2023a, Fig. 1).

To cover a range of elements with contrasting geochemical characteristics, i.e., Goldschmidt classification (Goldschmidt, 1937; White, 2018), we selected 13 trace metals (As, Cd, Cu, Mo, Ni, Pb, Re, Sb, Sn, Tl, U, V, Zn), comprising sulfide-affine (=chalcophile) elements (As, Cd, Cu, Mo, Ni, Pb, Sb, Sn, Tl, Zn), iron-affine (=siderophile) elements (Mo, Ni, Re, Sn), and silicate and oxide-affine (=lithophile) elements (Tl, U, V). Duplications of certain elements (Mo, Ni, Sn, Tl) in multiple groups arise in the estuarine–marine environment from variations in ambient pH, temperature, salinity, and redox conditions, affecting the metals dissolved and particulate speciation and oxidation state (Salomons et al., 1987; Gambrell et al., 1991; Du Laing et al., 2009; Bruland et al., 2014). For our investigating of trace metal–host phase behavior, we further considered three major elements (Al, Fe, Mn; representative of silicates, oxides, sulfides) and two non-metal solid phase constituents, sulfur (S; representative of sulfides), and total organic carbon (TOC; representative of OM). For each of the sites, sedimentary trace metal, S and TOC

contents from one sediment core (0–~30–60 cm length, 0.4–5 cm resolution; see Fig. S2 and Paul et al., 2023a for detailed sampling intervals per site) were included in the analysis. As we focus on the increasing sedimentary trace metal enrichments during the late-19th to mid-20th century, sediment core intervals representing much older time intervals (>200 years) were omitted from the analysis. This concerns the abyssal Black Sea, for which only the upper 10 cm were considered (~1850, Phoxy St. 2; Dijkstra et al., 2018). Sediment surface samples comprising fresh, unconsolidated, suspended OM (=“fluff layers” with exceptionally high TOC contents), present at Fårö Deep and the Northern Gotland Basin were also omitted from the analysis (van Helmond et al., 2018). For comparison, omitted samples are shown in the sediment core profiles (Fig. S2).

To assess whether our study sites are enriched in anthropogenic trace metals relative to natural background concentrations, we compare the sedimentary trace metal contents to ranges in background content, estimated from both local background and global Upper Continental Crust (UCC) values (Rudnick and Gao, 2014). Details on the background value estimation can be obtained from the Supplementary Material (Table S1).

### 2.2. Solid phase analyses

#### 2.2.1. Determination of total metal, S, and TOC contents

Solid-phase total metal and S data were determined using triple-acid (HF/HClO<sub>4</sub>/HNO<sub>3</sub>) digestion of O<sub>2</sub>-free sampled, (freeze)-dried, and homogenized samples from short sediment cores (0–~30–60 cm length; for site-specific core lengths see Fig. S2), and subsequent analysis of As, Cd, Cu, Mn, Mo, Ni, Pb, Re, Sb, Sn, Tl, U, V, and Zn by Inductively Coupled Plasma-Mass Spectrometry (ICP-MS) and Al, Fe, and S by Inductively Coupled Plasma-Optical Emission Spectrometry (ICP-OES), as described in Paul et al. (2023a). Further analytical details and instrument specifics can be obtained from the Research Data file available from Zenodo (<https://doi.org/10.5281/zenodo.12759164>).

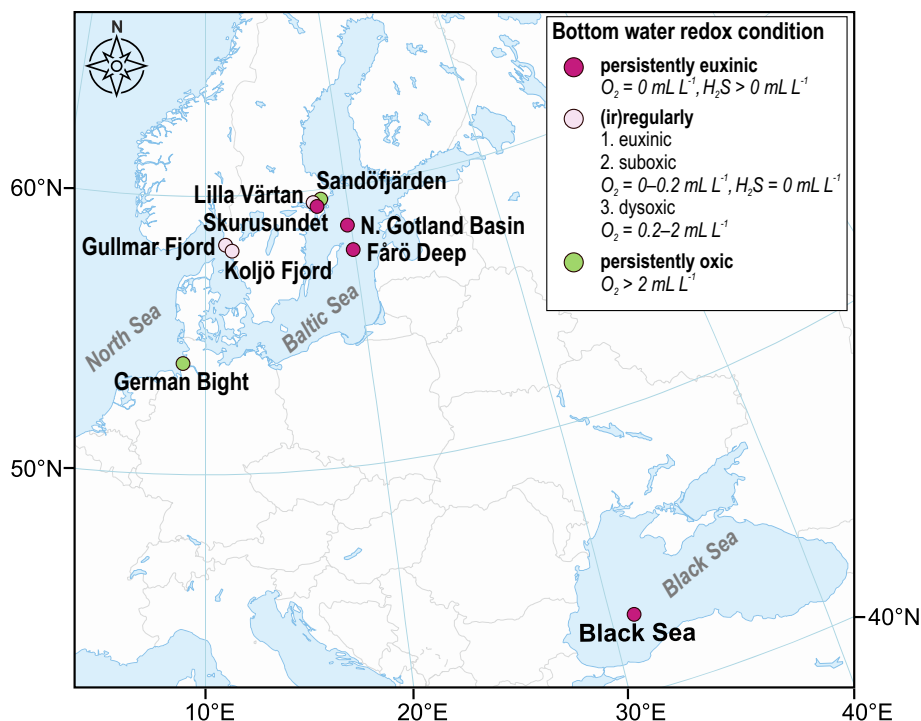


**Fig. 1.** Location of the nine study sites. The color of each study site refers to the modern average bottom water redox condition (dark pink = persistently euxinic; light pink = (ir)regularly dysoxic–euxinic; green = persistently oxidic). The redox categorization is adapted from Paul et al. (2023a). The map was modified from EEA (2021). Close-ups of the study sites at the Swedish west coast (Gullmar and Koljö Fjord), in the German Bight, and the Stockholm Archipelago, are provided in the Supplementary Material (Fig. S1).

**Table 1**

List of study sites, brief site description and trace metal pollution sources and history. Bottom water (BW) redox conditions, BW salinity, water depth and sedimentation rate according to Paul et al. (2023a).

BW Redox condition	Study site	Approx. deep-water mixing time	Water depth (m)	BW salinity	Average sedimentation rate (cm yr <sup>-1</sup> )	Brief summary of metal pollution sources (19th–21st century)	Main trace metal input pathway(s)	References
Baltic Sea – Eastern Gotland Basin								
Persistently euxinic	Fårö Deep	~30 years	191	12.0	~0.66	Emissions from fossil fuel-based (coal, oil) power production, intense ship- and leisure boat traffic	Atmospheric deposition waterborne (rivers + coastal run off)	Hallberg (1991) Borg and Jonsson (1996) Schneider et al. (2000) Stigebrandt and Gustafsson (2003) Ytreberg et al. (2022)
Persistently euxinic	Northern (N.) Gotland Basin	~30 years	169	11.4	~0.23			
Baltic Sea – Stockholm Archipelago								
Persistently euxinic	Skurusundet	2–4 years	27	5.3	~1.4	Mining in Bergslagen region (outflow via Lake Mälaren), local/regional emissions and (until 1960 untreated) sewage discharge from industries, power production, wastewater treatment plants, road traffic, leisure and commercial boat and ship traffic and harbor activities Influence: Lilla Värtan > Skurusundet > Sandöfjärden	Waterborne atmospheric deposition Waterborne atmospheric deposition Waterborne, atmospheric deposition	Broman et al. (1994) Engqvist and Andrejev (2003) Lehtoranta et al. (2022) Stockholms Vattenprogram (2011) SMHI (2022)
(Ir)regularly suboxic-dysoxic	Lilla Värtan	Spring and late fall–early winter (up to 6 months)	21	4.9	~1.9			
Persistently oxic	Sandöfjärden	Unrestricted towards the Baltic	64	5.8	~0.4			
Swedish west coast								
(Ir)regularly euxinic	Koljö Fjord	Usually annually, but up to 5–7 years	43	27.7	~0.40	Boat building industry on Orust, plastic boats since 1960s; presently local sources are assumed to negligible due to sparse population and industry density	Waterborne, atmospheric deposition	Gustafsson and Nordberg (1999) Nordberg et al. (2001) Larsson and Lindström (2014) SMHI (2022)
(Ir)regularly dysoxic	Gullmar Fjord	Usually annually	117	34.4	~0.62			
North Sea – Helgoland mud area								
Persistently oxic	German Bight	Unrestricted	30	32.2	~0.17 <sup>a</sup>	Mining activities (Harz Mountains and Erzgebirge), discharge via Elbe and Weser estuaries, remobilization, and deposition of contaminated sediments	Riverine, atmospheric deposition	Kersten et al. (1988) Irlon (1994) Boxberg et al. (2020)
Black Sea – NW abyssal plain								
Persistently euxinic	Black Sea	>200 m ~ 850 ± 300 years <sup>b</sup>	2107	22.3	~0.10	Emissions from fossil fuel-based (coal, oil) power production, intense ship- and leisure boat traffic	Atmospheric deposition, waterborne (riverine + coastal run off)	Top et al. (1990) Topcuoglu (2000) Murray et al. (1991) Lee et al. (2002) Theodosi et al. (2013)

<sup>a</sup> Sedimentation rate was re-estimated from Paul et al. (2023a) based on Boxberg et al. (2020). For details see Section 2.3.

<sup>b</sup> Averaged based on the sources provided in the references.

Accuracy (recovery) of all new data was based on in-house standards and the commercial sediment reference material ISE-921 were between 89 and 114 % for all elements analyzed on the ICP-MS (all except Fe and S). For Fe and S recoveries were between 91 and 127 %, and 82–110 %, respectively. The precision (relative standard deviation, RSD %) based on sediment sample duplicates was between 2 and 10 % for all elements, except for Cu (13 %), Sb (20 %), and Tl (19 %) for the three Stockholm Archipelago sites.

Total organic carbon (TOC) was determined after decalcification and drying and analyzed via thermal combustion. Total trace metal- and TOC contents were corrected for salt-dilution using the bottom water

salinity and sediment porosity, assuming a solid-phase density of 2.65 g cm<sup>-3</sup> (Burdige, 2006). Some of the here presented solid phase data has been previously published; further details regarding those are provided in Table 2.

### 2.2.2. Data normalization and statistical analysis of metal, S, and TOC contents and covariation patterns

In our analyses we use unnormalized solid phase data instead of normalizing them against the detrital background (=Al content). While the latter is a common practice to recover authigenic (non-lithogenic) signals from dilution by the detrital fraction of a given element (e.g.,

**Table 2**  
References of the solid-phase metal, major element, TOC, and S data.

Study site	Mo, U	Al, As, Cd, Cu, Ni, Mn, Pb, Re, Sb, Sn, Tl, V, Zn	TOC	Fe, S
Fårö Deep & N. Gotland Basin	Jilbert and Slomp (2013a, 2013b) van Helmond et al. (2018)	van Helmond et al. (2018) <i>Sn: This study</i>	Jilbert and Slomp (2013a, 2013b) Lenz et al. (2015)	Jilbert and Slomp (2013a, 2013b) Lenz et al. (2015)
Stockholm Archipelago	Paul et al. (2023a)	<i>This study</i>	Paul et al. (2023a)	<i>This study</i>
Koljö- and Gullmar Fjord	Paul et al. (2023a, 2023b)	<i>This study</i>	Paul et al. (2023a, 2023b)	<i>This study</i>
German Bight	Paul et al. (2023a)	<i>This study</i>	Paul et al. (2023a)	<i>This study</i>
Black Sea	Paul et al. (2023a)	<i>This study</i>	Kraal et al. (2017)	Kraal et al. (2017)

Tribovillard et al., 2004; Böning et al., 2015; Bennett and Canfield, 2020), under certain environmental settings, e.g., with a small detrital fraction size or variable detrital source material, this method may result in “spurious” correlations (Van der Weijden, 2002). Following Van der Weijden (2002), we calculated the coefficients of variation (CV = standard deviation divided by the mean) of Al (CV<sub>Al</sub>), the trace metals, S, and TOC (CV<sub>x</sub>) for each site ( $n = 9$ ) to assess the potential risk of Al-normalization. We found relatively large variation across our study sites and elements but generally low CV<sub>Al</sub> and CV<sub>x</sub> > CV<sub>Al</sub>. Thus, we believe that for our specific study, unnormalized data provide a more reliable estimate of the trace metal and S, and TOC contents than Al-normalized contents. Ranked Al-normalized trace metal ranges can be obtained from the Supplementary Material (Fig. S6).

Variability in total trace metal, S, and TOC contents between sites was estimated by comparing their Median Absolute Deviation (MAD, e.g., Pham-Gia and Hung, 2001), and 0.95 confidence intervals (CIs) of the mean, using the bootstrapping resampling method (e.g., Carpenter and Bithell, 2000). This approach is suitable for non-normally distributed data containing small (sub)sample sizes and outliers (e.g., “fluff” surface sediments, Section 2.1) (Rowland et al., 2021), both of which apply to our data. Overall, narrower MAD and CI ranges indicate a more reliable and generalized distribution pattern of the data.

For investigating the frequency and importance of inter-metal, S-metal, and TOC-metal relationships across our study sites, we computed the correlation coefficients of the content data of each element pair and summarized these as correlation matrices. For each elemental pair, the 0.95 CI and  $p$ -values were calculated to test whether the correlation coefficient (positive or negative) is significant. Finally, all positive and significant correlations ( $p < 0.05$ ) per site were manually counted and summarized in a single meta-matrix to identify and differentiate between site-dependent and site-independent correlations. All matrices were ordered according to the number of positive correlations in the summed meta-matrix, in which Pb was identified as the primary element, i.e., with the highest overall number of sites reporting significant correlations for a Pb-element pairs. Violin plots comparing individual sites were also arranged in order of Pb content.

Computation and visualization were performed in R (version 4.2.3). For the violin plots and calculation of MADs and CIs we used the *ggplot2* package with the *geom\_violin()* and *stat\_summary()* functions. For correlation matrices we used the *corrplot* and *hmisc* packages.

### 2.3. Sediment core chronologies

Age-depth models based on <sup>210</sup>Pb and <sup>137</sup>Cs, respectively, were available for the study sites in the Black Sea (Dijkstra et al., 2018), central Baltic Sea (Jilbert and Slomp, 2013a), Stockholm Archipelago

(Paul et al., 2023a), and Swedish west coast fjords (Nordberg et al., 2000; Filipsson and Nordberg, 2004; Paul et al., 2023b). For the German Bight site, we approximated an age model using a combination of an existing <sup>210</sup>Pb and <sup>14</sup>C-based average sedimentation rates from nearby sediment cores (GeoB4806-1 and GeoB 4801-1) and the dated onset of industrial Zn pollution (~60 mg kg<sup>-1</sup>) in the area (~1850, Hebbeln et al., 2003; Boxberg et al., 2020). Zinc contents in our core are consistently elevated at >60 mg kg<sup>-1</sup>, thus we assume that our sediment core covers an interval between >1850 and 2019, giving a minimum sedimentation rate of 0.17 cm yr<sup>-1</sup>.

## 3. Results

### 3.1. Sedimentary trace metal distribution and correlation patterns

Median sedimentary Pb contents are highest at the persistently euxinic Skurusundet site in the inner Stockholm Archipelago (~145 mg kg<sup>-1</sup>) and lowest at the persistently euxinic abyssal Black Sea site (~19.5 mg kg<sup>-1</sup>) (Fig. 2). Only Sn follows a similar ranking of sites as Pb, while Cd, Cu, Zn, Sb, Ni, As, and Tl show a distinct ranking pattern, with relatively elevated values in the persistently euxinic Fårö Deep and N. Gotland Basin sites. Lead, Cd, Cu, Zn, Sb, Sn, and As are at most sites enriched relative to their background values (gray shaded area, Fig. 2), whereas for Ni, Tl, V, Mo, U, and Re no consistent enrichment pattern is observed. According to the summed meta-matrix, sedimentary trace metals broadly cluster in two groups (Fig. 3): (I) trace metals with positive and significant correlations at ≥ five sites (blue colors: Pb, Cd, Cu, Zn, Sb, Sn, Ni, As, Tl) and (II) trace metals with positive and significant correlations at < five sites (orange-red colors: V, Mo, U, Re). Among group (I), Pb and Zn have the highest count of positive correlations across the study sites to each other, Cd and Cu (nine sites), within group (II) Mo and U are more frequently correlated to each other than to Re and V. Intercorrelations between groups (I) and (II) are relatively rare, except for Zn, Sb, Ni, and As, which are positively correlated to both Mo and U at 5–9 sites (Figs. 3, S4) and together with Cd and Tl also share common features in ranked trace metal enrichment pattern (Fig. 2). On the site-scale, correlation frequency and correlation strength between the trace metals differs quite considerably (Fig. 4).

### 3.2. Total S and organic carbon distribution and correlation patterns

Median S and TOC contents are lowest for the open marine and oxic German Bight (0.4 wt% S and 1.1 wt% TOC). While elevated contents (>1 wt% S and 5 wt% TOC, respectively, Fig. 2), also occur at less reducing and non-euxinic sites (e.g., Sandöfjärden and Lilla Värtan), highest S and TOC contents are exclusively found at sites with euxinic bottom waters, irrespective of water depth, salinity, and distance to shore. For S, this concerns the relatively shallow and (ir)regularly euxinic Koljö Fjord (2.4 wt% S) and the persistently euxinic, abyssal Black Sea site (2.0 wt% S), while for TOC, this concerns the persistently euxinic Fårö Deep (8.3 wt. TOC %) and Skurusundet (8.0 wt% TOC; Fig. 2, Table 1). Correlation coefficients of TOC and S to the other variables are very heterogenous across the study sites, although they share positive and significant correlations with Ni and Sb (Fig. 3). Overall, TOC is positively correlated with most trace metals (and most frequently with Cd and Zn), whereas S is only commonly associated with Sb, Ni, Mo, and Fe (Fig. 3).

## 4. Discussion

### 4.1. Grouping of trace metals

Our summed meta-matrix shows a division of the trace metals into two groups (I, II) (Section 3.1, Fig. 3), very well matching with the primary sources and geochemical controls of the trace metals contributing to excess enrichments in the marine environment. Group (I) trace

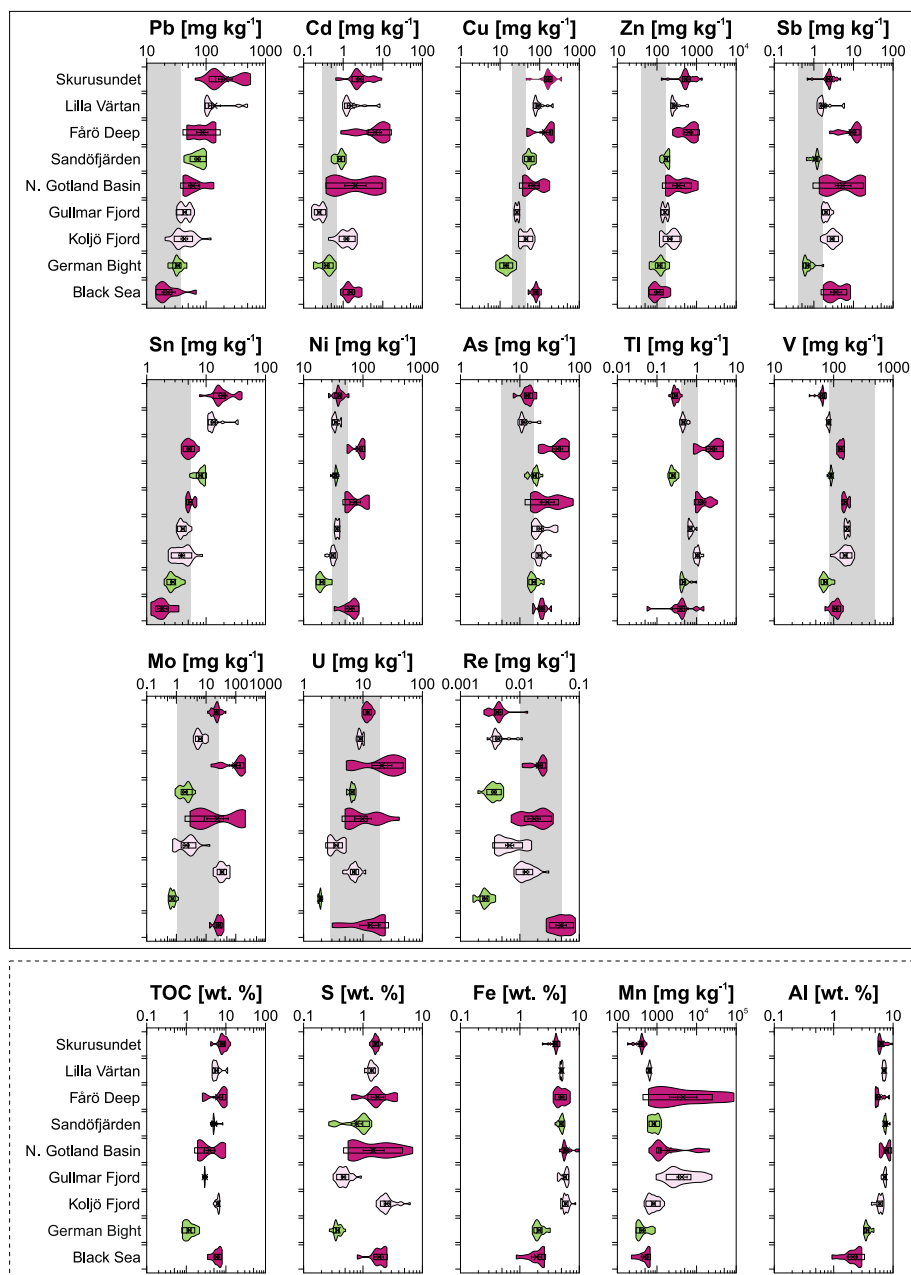


**Fig. 2.** Total content ranges of the 13 trace metals (solid frame), and sedimentary host phases (dashed frame) across the nine study sites, displayed as violin plots and transformed into  $\log_{10}$  scale. Each violin includes the mean (black solid crosses), 0.95 confidence interval (CI) of the mean (whiskers), median (vertical solid black line), and the median absolute deviation (MAD, crossbar). For the color coding see Fig. 1 legend and caption. Natural background contents are given as references (gray shaded area); note: minimum background values for Pb and Sn are 8 and 0.8  $\text{mg kg}^{-1}$ , respectively. For details on the determination of the background ranges, see Section 2.1 and Table S1. Organic-rich “fluff layers” were omitted from the analyses.

metals (Pb, Cd, Cu, Zn, Sb, Sn, Ni, As, Tl) are largely derive from anthropogenic sources (Nriagu, 1989; Bruland et al., 2014), and thus “anthropogenically sourced” trace metals. Contrary, for group (II) trace metals (Mo, U, Re, and V), anthropogenic sources (e.g., mining, oil and coal combustion, phosphate fertilizer, Colodner et al., 1995; Reimann and De Caritat, 1998; Pacyna and Pacyna, 2001), likely have a minor contribution to the total sedimentary loading. Instead, the degree to which Mo, U, V, and Re are enriched in (coastal) marine sediments is believed to be mainly driven by their natural geochemical behavior in seawater as a function of redox variability (e.g. Morford and Emerson, 1999; Tribovillard et al., 2006; Bennett and Canfield, 2020), making them “redox-sensitive” trace metals. Following this categorization, the site-wide positive correlations between the anthropogenically sourced

(I) metal pairs Pb—Cd, Pb—Cu, Pb—Zn, Zn—Cd, and Zn—Cu can at first order be explained by their co-occurrences in anthropogenic sources and primary deposition via airborne (atmospheric) or waterborne (fluvial) pathways. For example, in terrestrially sourced aerosols from fossil fuel combustion (Pb, Zn, Cu) and metal industry (Pb, Zn, Cu, Cd), or local fluvial (point) sources from discharge of sewage sludge (Pb, Cd, Cu), battery production (Ni, Cd), corrosion of ship and automobile parts (Pb, Cu, Zn), and applications in agriculture (Cu, Zn) (Nriagu and Pacyna, 1988; Reimann and De Caritat, 1998; Pacyna and Pacyna, 2001; Callender, 2014 and references therein). If anthropogenic trace metal distribution in coastal marine sediments were primarily controlled by sharing common sources, these trace metal pairs (Pb—Cd, —Cu, —Zn, Zn—Cd, and Zn—Cu) should also show similar distribution patterns

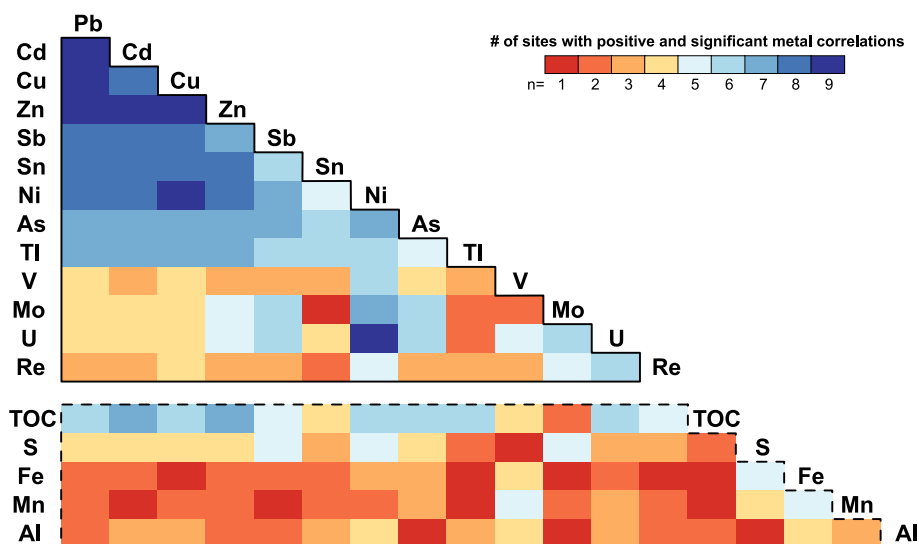


**Fig. 3.** Summed correlation matrix ranked after Pb. The colors correspond to the number of sites (1–9) that have a positive and significant correlation for a given element, whereby 9 is the maximum (=nine sites) and 1 the minimum (=one site). The dashed border highlights trace metal-host phases correlations (OM compounds = TOC, sulfides = S, Fe and Mn oxides = Fe and Mn, and silicates/clay minerals = Al).

across the study sites, irrespective of the distance from shore and other depositional environmental factors.

However, when comparing the summed meta-matrix grouping with the ranked trace metal enrichment pattern across the study sites, the close correlation between Pb and Cd, Cu, and Zn observed in the meta-matrix (Fig. 3) is absent in the ranking (Fig. 2). Instead, Pb and Sn appear to be stronger correlated to each other by following almost the same ranked range pattern (Fig. 2), having the greatest site-wide correlation coefficient (0.91; Fig. S4), yet they are not positively correlated at all sites (Fig. 3). These apparent discrepancies suggest that sedimentary enrichment and covariation patterns in (near) coastal sediments between anthropogenically sourced trace metals are not only dictated by deriving from similar anthropogenic sources but are co-controlled by secondary factors.

The significance of secondary factors in the applicability and reliability of (II) redox-sensitive trace metals as redox proxies includes the presence and intensity of the Fe and Mn oxide shuttle,  $H_2S$  concentration in the bottom- and pore water, and post-depositional oxidative remobilization (Zheng et al. (2002); Algeo and Lyons, 2006; Algeo and Tribouillard, 2009; Jokinen et al., 2020b; Helz, 2021, 2022; Paul et al., 2023a, 2023b). In the following, we investigate the most significant secondary factors in explaining site-wide and site-specific correlation and distribution patterns, similarities, and divergences among group (I) trace metals.

We acknowledge that dilution effects caused by vertical variability in the sediment composition (e.g., grain size and carbonate contents) may also influence the distribution and contents of certain trace metals (Smrzka et al., 2019). Among our nine study sites, we expect that only at German Bight and Black Sea Abyssal Plain such dilution effects may be observed due to the presence of fine sand in the upper 8 cm of the German Bight sediments and high carbonate contents (>30–50 wt%; Kraal et al., 2017) in Black Sea sediments. However, we consider them not to have a stronger influence on trace metal distribution relative to the other factors discussed in this study.

## 4.2. Secondary factors influencing trace metal sequestration

### 4.2.1. Sulfide mineral formation

Overall, the anthropogenically sourced trace metals Pb, Cd, Cu, Zn, Sb, Sn, Ni, As, Tl are more strongly enriched in sediments deposited under persistently euxinic conditions (dark pink sites) than under oxic conditions (green sites) (Fig. 2). This pattern can be related to the

solubility of the trace metals' host phases after deposition on the seafloor (Calvert and Pedersen, 1993). The above trace metals behave highly chalcophile upon  $H_2S$  release into the bottom- and/or pore water following microbial mediated organo-clastic sulfate reduction or anaerobic oxidation of methane (AOM, Jørgensen et al., 1990, 2019), by either precipitating as refractory native sulfide minerals (e.g., PbS, CdS, ZnS,  $CuS_2$ ) or co-precipitating with other (Fe)-sulfide minerals, such as iron-monosulfide (FeS) or pyrite ( $FeS_2$ ) (e.g., Cu, Ni, As, Sb; Salomons et al., 1987; Huerta-Diaz and Morse, 1992; Billon et al., 2001; Tribouillard et al., 2006; Tribouillard, 2020; Canavan et al., 2007). Positive correlations between these metals and S and Fe at the euxinic sites Fårö Deep (Fig. 4C), and N. Gotland Basin (Fig. S5), and most strongly for Ni at the abyssal Black Sea site (Fig. S5) are indicating the presence of such trace metal-host phase associations.

Additional positive correlations to S (and Fe) are found at the seasonally dysoxic-suboxic (sometimes euxinic) Lilla Värtan but also at the persistently oxic Sandöfjärden (Fig. 4A). The latter is surprising due to its non-reducing bottom water redox conditions, under which sulfides typically do not precipitate or are readily dissolved (Kerner and Wallmann, 1992; Outridge and Wang, 2015), as seen at German Bight by lowest S contents and decoupling to trace metals. By contrast to the German Bight, at Sandöfjärden, and the Stockholm Archipelago in general, formation and preservation of sulfide minerals in the sediment is permitted by the combined effect of low salinity (Table 1) and eutrophic conditions (van Helmond et al., 2020a; Dalcin Martins et al., 2024), leading to compression of the diagenetic zonation (Canfield and Thamdrup, 2009) and an upward migration of the intensive  $H_2S$  production zone (Slomp et al., 2013; Rooze et al., 2016; Wallenius et al., 2021) to shallow sediments (Dalcin Martins et al., 2024). Similar observations have been previously reported for sites in the Bothnian Sea (Egger et al., 2015; Rasigraf et al., 2020) and Finnish Archipelago Sea (Jilbert et al., 2018; Jokinen et al., 2020b), and are linked to higher trace metal sequestration and preservation potentials (Ingri et al., 2014; Jokinen et al., 2020a, 2020b).

Decoupling between trace metals and S is not restricted to oxic sites, as shown by the correlation matrix of the (ir)regularly euxinic Koljö Fjord (Fig. 4B). Although scavenging and formation of trace metal (Fe)-sulfide phases is generally permitted under the sulfidic pore water, short and long-term rapid redox variations in the bottom and pore water can lead to metal remobilization and loss of correlations between metals and host phases that were originally preserved, as previously described for Mo at this site (Paul et al., 2023b).

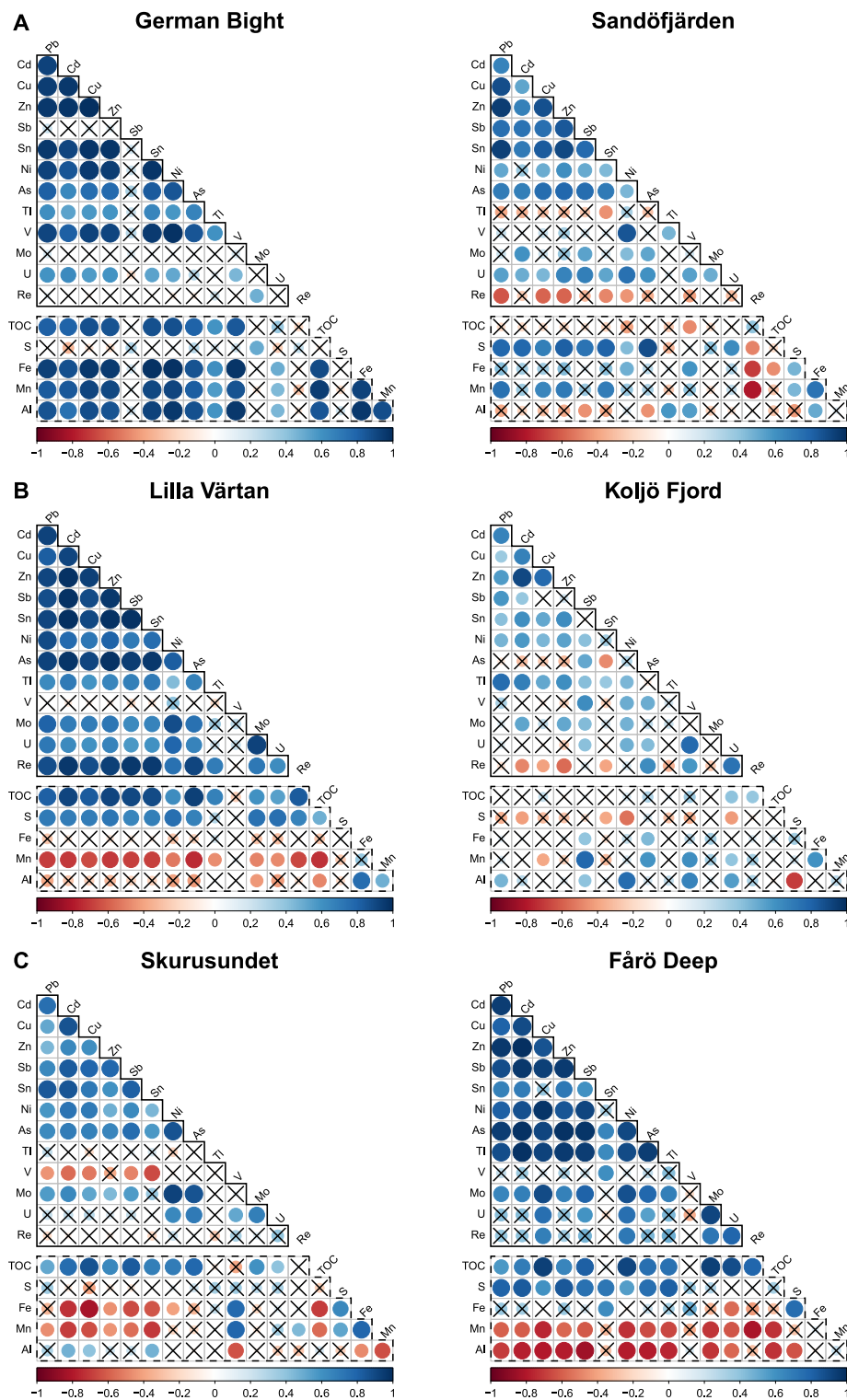


**Fig. 4.** Comparison between correlation matrices of two A) oxic B) (ir)regularly dysoxic–euxinic, and C) persistently euxinic sites. The color of each circle indicates whether the correlation is positive (blue) or negative (red). Color intensity and circle size are proportional to the correlation coefficients (–1 to 1). Correlations with  $p < 0.05$  are considered insignificant and marked with an X. Color intensity and size of each circle are proportional to the correlation coefficient, i.e., the more intense the color and larger the size, the stronger the correlation (positive or negative). The dashed border highlights trace metal–host phases correlations (cf. Fig. 3 caption).

#### 4.2.2. Trace metal–OM associations

Refractory OM is an important host phase of trace metals in sediments (Calvert and Pedersen, 1993; Bruland et al., 2014). Our data show positive and significant correlations of Pb, Cd, Cu, Zn, Sb, Sn, Ni, As, Tl with TOC at 4–7 sites across a range of redox conditions (Figs. 3, 4, S5), implying that delivery of refractory OM to sediments may serve as a

secular variable modulating trace metal enrichment. Allochthonous (terrestrial) OM is more refractory than phytoplankton-derived (autochthonous) OM (Callender, 2000) and trace metals such as Pb, Cu, Cd, Zn, Ni and Sn have a high affinity for associating with allochthonous OM in estuarine settings (Nordmyr et al., 2008a, 2008b; Karbassi et al., 2013; Jokinen et al., 2020a; Virtasalo et al., 2023). This

association provides a mechanism for simultaneous delivery of metals and OM to sediments in coastal areas. Salinity-induced flocculation of dissolved OM (DOM) into particulate OM (POM) at the land-sea transition, where freshwater mixes with seawater (Boyle et al., 1977), favors sedimentation of OM and associated trace metals in relatively close proximity to freshwater outlets (Puls et al., 1997; Sholkovitz, 1978; Palanques et al., 1995; Nordmyr et al., 2008a, 2008b; Karbassi et al., 2013; Virtasalo et al., 2023). Of all study sites, Lilla Värtan has the highest correlation coefficients between anthropogenically sourced trace metals and TOC (average  $\approx 0.83$ ; Fig. 4B), while at the nearby Skurusundet, almost all anthropogenically sourced trace metals are positively correlated to TOC, while being decoupled from Fe and S (Fig. 4C). This finding stands in stark contrast to the other euxinic sites, where trace metals are dominantly associated with sulfides (Figs. 4, S4).

The strong correlations between TOC and trace metals in the Stockholm Archipelago sites may be induced by DOM flocculation and subsequent sedimentation occurring in close proximity to the freshwater outlet of Lake Mälaren, which is a key supplier of allochthonous OM to the archipelago (Broman et al., 1994; Lehtoranta et al., 2022). Interestingly, the inner Stockholm Archipelago shows the highest contents of Pb and Sn, and elevated contents of Cu and Zn, whereas Sb, Ni, As, Tl, and Cd contents are higher in the offshore stations in the central Baltic Sea (Fårö Deep and N. Gotland Basin, Fig. 2). This pattern may be related to relative loading of the different metals from anthropogenic activities but also potentially to incongruent association of metals to different fractions of OM that are prone to sedimentation or long-distance transport depending on the degree of aggregation, as discussed for continental margins (Lenstra et al., 2022), and estuarine settings (Böning et al., 2017).

#### 4.2.3. Particulate Fe and Mn oxide shuttling

Iron- and Mn oxide recycling is a well-known and important mechanism for efficiently shuttling redox-sensitive (Mo, V; e.g., Morford and Emerson, 1999; Scholz et al., 2013) and anthropogenically sourced trace metals (As, Sb, Cu, Ni, Zn, Pb; e.g., Salomons et al., 1987; Tribouillard et al., 2006; Tribouillard, 2021; Little et al., 2015) to surface sediments of various coastal (marine) environments worldwide, including our study sites (Fårö Deep and N. Gotland Basin: Jilbert and Slomp, 2013b; van Helmond et al., 2018; Gullmar- and Koljö Fjord: Goldberg et al., 2012; Paul et al., 2023b; German Bight: Slomp et al., 1997). Yet, our correlation matrix shows very low numbers of positive trace metal to Fe or Mn correlations, which are largely restricted to the German Bight, the most oxic site (Fig. 4A).

In fact, we observe that Gullmar Fjord, Lilla Värtan, Skurusundet, and Fårö Deep show significant negative correlations for many trace metals assumed to be associated with Fe and Mn oxides (Figs. 4, S4). We attribute this apparent decoupling to the behavior of labile Mn and Fe oxides at the oxic-suboxic redox transition close to the sediment surface (Burdige, 1993). In this regime, vertical refluxing of dissolved Fe and Mn in pore waters can lead to enrichments of Fe and Mn oxides in the upper sediments (Fig. S2A, Burdige, 1993; Adelson et al., 2001; Sulu-Gambari et al., 2017). Trace metals transported to the sediments adsorbed to these oxides may be released to pore water during oxide reduction, and re-scavenged by newly formed oxides from non-Mn reducing pore water (e.g., German Bight, Fig. S2), or are scavenged by more refractory carrier- and host phases, such as sulfides, carbonates, phosphates, or clay minerals (e.g., Salomons et al., 1987; Scholz and Neumann, 2007; Dang et al., 2015). This can lead to enrichments of Fe and Mn at the core top and of trace metals deeper in the core, causing poor or negative correlations between Fe and Mn and associated trace metal contents in our data (e.g., Figs. 3, 4, S4). A similar mechanism has been used to explain offsets of trace metal enrichments from Mn-rich layers in sediment cores following intermittent oxygenation events (Scholz et al., 2018).

Due to the mechanism outlined above, we infer that negative correlations between Fe, Mn and trace metals may in fact serve as a measure for identifying active Fe and Mn oxide shuttling at a given study site. By

extension, positive trace metal-Fe and/or Mn correlation may either be indicative of deposition under weakly reducing/oxic conditions or represent co-occurrences in secondary trace metal carrier- and host phases, which often contain Mn and Fe (e.g., pyrite, rhodochrosite, siderite, vivianite) and are known to make up a considerable fraction of the Fe and Mn in the sediment at some of our study sites (Fårö Deep, N. Gotland Basin, abyssal Black Sea, Sandöfjärden; Jilbert and Slomp, 2013b; Dijkstra et al., 2018; Dalcin Martins et al., 2024). In this context, the considerable Sb, Ni, As, and Tl enrichments at Fårö Deep and N. Gotland Basin (Fig. 2) may be a consequence of direct trace metal input through long-distance transport, the efficiency of the particulate shuttle, and permanent burial in secondary host phases under reducing conditions (Lenz et al., 2015; van Helmond et al., 2018). The significance of this combined mechanism for promoting trace metal sequestration becomes more apparent when compared to sites that either have an extremely large Mn oxide pool but insufficient sulfide production in the pore water impeding permanent trace metal sequestration (Gullmar Fjord; Brinkmann et al., 2023; Paul et al., 2023b), or have a persistently sulfidic water column (abyssal Black Sea), permitting the precipitation of sulfide minerals but limiting the efficiency of the Fe and Mn oxide shuttle, and thus trace metal transport, (Lenstra et al., 2019, 2020) below the chemocline ( $\sim 150$  m; Huang et al., 2000; Eckert et al., 2013).

#### 4.3. Proxy potential of anthropogenic trace metals in coastal marine sediments

##### 4.3.1. The 1970s atmospheric Pb peak: where can we find it, where not, and why?

Considering the secondary factors outlined in the previous sections, Pb appears to be the trace metal with the highest potential to record the history of direct pollution to any given sedimentary location, due to its relative particle reactivity and post-depositional immobility. We investigated the extent to which our Pb profiles match the timing of the commonly reported 1970s sedimentary Pb peak observed in northern/western Europe and North America across various coastal marine, estuarine, lake, soil, and peat sediments. This peak has been previously related to atmospheric deposition of Pb as a consequence of leaded-gasoline emissions and is often used as an age marker in environmental reconstructions (Valette-Silver, 1993; Shotyk et al., 1998; Brännvall et al., 2001; Zillén et al., 2012; Jokinen et al., 2020a; van Helmond et al., 2020b; Renberg et al., 2001a).

According to our core chronologies (Section 2.3, Fig. 5), the only three sites showing marked enrichment peaks in Pb during the 1960s–70s (Table S1; Zillén et al., 2012; van Helmond et al., 2018) are the two deep Baltic Proper sites (Fårö Deep and N. Gotland Basin), and the abyssal Black Sea. Such offshore sites are expected to be primarily impacted by atmospheric deposition of anthropogenically-sourced trace metals (Suess and Erlenkeuser, 1975; Hallberg, 1991; Topcuoglu, 2000; Theodosi et al., 2013), hence the observations match the expected profiles from literature. In contrast, many of the nearshore sites show maximum Pb contents preceding the 1970s by at least half a century. The German Bight even shows a reverse trend with increasing Pb contents from 1900 until present with maximum contents in the upper 10 cm (Fig. 5). Although explanations for indistinctly developed or missing 1970s atmospheric Pb peaks have been addressed previously for sedimentary lake, bog, and other coastal records (Farmer, 1991; Valette-Silver, 1993; Renberg et al., 2001a; Carignan et al., 2003; Outridge and Wang, 2015), they have not been explored for our study sites, which cover a relatively large and diverse set of sedimentary records.

The absence of a clear “atmospheric” 1960s–70s Pb peak at nearshore sites implies that Pb profiles in these settings are related to local Pb pollution history derived from fluvial sources, including industrial point sources. For example, the Stockholm Archipelago has a several century-long history of regional and local trace metal pollution waterborne point sources from extensive pre-industrial (Pb, Cu, Zn ore) mining operations (Bergslagen region in the 10th–mid-20th century; Renberg et al., 2001a,

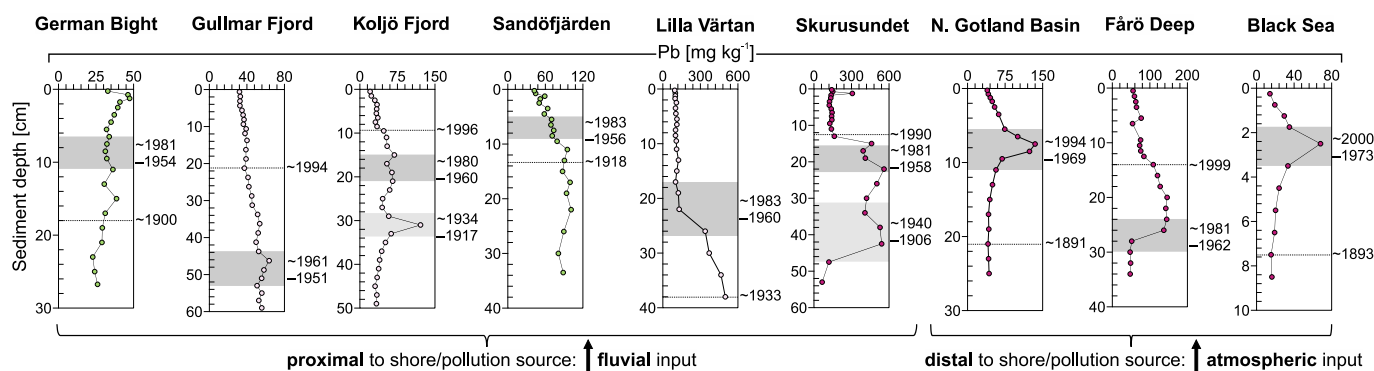


**Fig. 5.** Sediment Pb profiles at each study site. The color of the symbols corresponds to the sites average bottom water redox condition (cf. Fig. 2). Dark gray shaded areas denote the expected timing of the 1970s peak. Additional Pb peaks preceding the 1970s peak are highlighted by a light gray area. Distinct age markers are provided as reference, based on the core chronologies (Section 2.3). The sites were grouped with respect to the distance offshore and expected dominance of pollution input pathway, i.e., fluvial vs. atmospheric.

2001b; Olsson, 2007; van Helmond et al., 2020b), and other urban and industrial activities in the area (boat yard activities, paper- and pulp mills, discharge of unfiltered wastewater; Cederqvist et al., 2020; Norrlin et al., 2022; EBH-kartan (EBH Map), 2023). Also in the Gullmar Fjord and Koljö Fjord areas, several industrial activities may have contributed metal pollution (e.g., Munkedal paper and sulfite pulp mills; Lysekil herring canning industry; Leppäkoski, 1968, Rosenberg, 1990; Harland et al., 2006), boat yard activities (Orust area; Larsson and Lindström, 2014), and petrochemical industries (Stenungsunds area, southern part of Koljö Fjord; Cato, 2006). For the German Bight near-shore site, although atmospheric fallout is a significant source of many trace metals in this area (Kersten et al., 1988), the contribution of riverine derived Pb (from the adjacent Elbe and Weser River estuaries) is at least an order of magnitude higher (Boxberg et al., 2020). Further alternation of the German Bight profile may arise from sediment mixing as a result of biogenic (bioturbation), abiotic natural (wind-, wave-, and tidal dynamics, storm events, currents) and anthropogenic (bottom trawling, dredging) disturbances. Such processes have been shown to mix deposited sediments as deep as 20 cm (Irion, 1994; Boxberg et al., 2020), leading to smoothing of signals over decimeter-scale intervals (Goldberg et al., 1978; Outridge and Wang, 2015).

Notably, as clearly shown in Fig. 2, the absolute sedimentary Pb contents in nearshore settings can be much higher than in offshore sites. Our findings demonstrate that the large-scale atmospheric Pb deposition signal related to the combustion of leaded fuel may be masked in near-coastal sediments by preceding or coinciding heavy local waterborne Pb pollution sources (Renberg et al., 2001a). Therefore, with greater distance from shore, and greater water depth, the net influence of atmospheric Pb deposition increases (e.g., Hallberg, 1991; Theodosi et al., 2013), whereas at near-shore coastal sites, profiles more likely reflect local Pb pollution signals from industrial and urban anthropogenic pollution sources. In either case, persistently euxinic conditions may promote the preservation of the Pb pollution signal through facilitating Pb uptake into sulfides and thus reducing post-depositional remobilization (Goldberg et al., 1978; Farmer, 1991; Valette-Silver, 1993; Outridge and Wang, 2015), although the low solubility of Pb across a wide range of redox conditions allows it to be retained in less reducing settings as well (Gambrell et al., 1991; Calmano et al., 1993).

#### 4.3.2. Redox proxy potentials of anthropogenic trace metals

Sedimentary Mo and U contents are the most widely applied redox proxies for ancient and modern aquatic environments (Algeo and Lyons, 2006; Algeo and Tribovillard, 2009; Scott and Lyons, 2012; Bennett and Canfield, 2020; Paul et al., 2023a). Although sedimentary Mo and U sequestration may also be influenced by pre- and post-depositional secondary factors (c.f. Section 4.1), significant differences in median Mo and U contents demonstrate their applicability as redox proxies

when multiple study sites are grouped according to their average modern bottom water redox condition (Paul et al., 2023a).

In recent decades, several transition metals (As, Cd, Cu, Ni, Sb, Zn, but particularly V and Re), have received increasing attention as potential redox proxies (either as bimetal ratio, enrichment factor, or ratio to TOC) due to their natural authigenic enrichment under reducing conditions (e.g., Calvert and Pedersen, 1993; Crusius et al., 1996; Algeo and Maynard, 2004; Algeo and Liu, 2020; Bennett and Canfield, 2020; Tribovillard, 2020, 2021; Vollebregt et al., 2023), and higher sensitivity in the oxic-dysoxic redox transition (Re, V; Morford and Emerson, 1999). Based on the data from the present study, we re-assess the applicability of As, Cd, Cu, Ni, Sb, Zn, V, and Re as redox proxies, by comparison with content ranges for Mo and U across representative sites in three redox bins (Fig. 6). To be considered valid as a potential proxy, median values for any given redox bin should not considerably overlap with the MAD crossbar and median of an adjacent redox bin (Section 2.2.2). As demonstrated by Paul et al. (2023a), oxic sites with a shallow sulfate-methane transition zone (SMTZ) may obscure the reliability of Mo- and U-based redox proxies by reflecting rather dysoxic-suboxic than oxic conditions. Of the sites in the present study, Sandöfjärden falls into this category. Therefore, we ran the analysis both including Sandöfjärden (gray, Fig. 6) and with only German Bight as an oxic endmember not influenced by geochemical trace metal processed related to a shallow SMTZ (green, Fig. 6).

The results show that As and V ranges severely overlap between the redox bins (Fig. 6), thus making them the least reliable and advisable candidates as independent redox proxies. Our findings support previous concerns regarding their redox proxy reliability (Cole et al., 2017; van Helmond et al., 2018; Bennett and Canfield, 2020; Tribovillard, 2020). Strikingly, Re also shows a poor reflection of the redox bins, with contents at euxinic Skurusundet (Fig. 2) similar to those at oxic sites. With regards to Skurusundet, our data show very similar Re contents across all Stockholm Archipelago sites (medians, oxic-euxinic: 3.67, 3.96, 4.33  $\mu\text{g kg}^{-1}$ , Fig. 2). Possibly, low Re contents are induced by low dissolved Re concentrations due to low ambient salinity (Colodner et al., 1993; Bura-Nakić et al., 2021). Similarly low sedimentary Re contents in the Bothnian Bay (Ingri et al., 2014) support this explanation. Alternatively, very high sedimentation rates at Skurusundet (and Lilla Värtan) may limit Re sequestration in surface sediments, since Re is largely transported into the sediment by diffusion (e.g., Colodner et al., 1995; Morford et al., 2005; Liu and Algeo, 2020). Although we cannot determine the ultimate factor(s) responsible for the observed Re features, our data indicate that in similar (low salinity-high OM loading, “estuarine-type”) depositional environments, e.g., estuaries, fjords, archipelagos, the redox proxy potential of Re may be hampered. Extraordinarily high Re contents at the abyssal Black Sea site (~2.5 times higher compared to the two euxinic Baltic Proper sites; Fig. 2) are likely the result of the

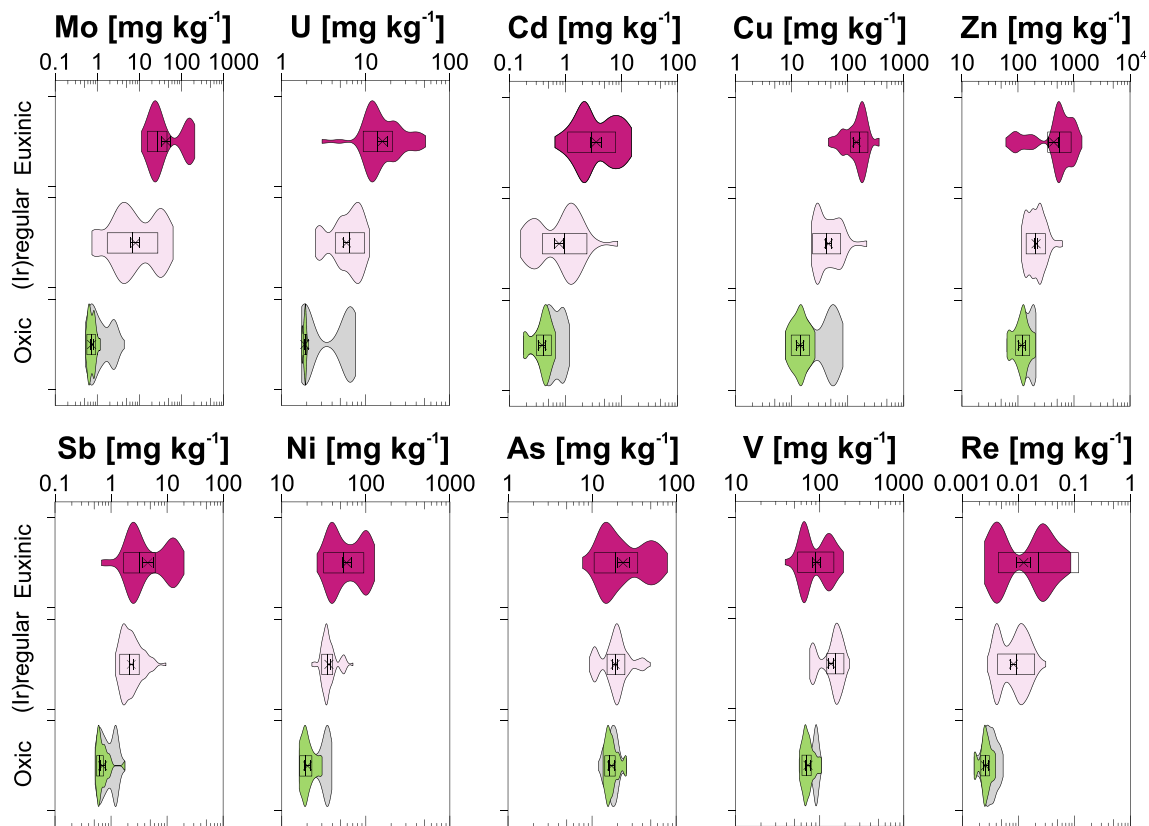


**Fig. 6.** Enrichment ranges of Cd, Cu, Zn, Sb, Ni, As, V, and Re compared to the redox proxies Mo and U across the study sites, binned according to their bottom water redox conditions (Fig. 1, Table 1): persistently euxinic (dark pink), (ir)regularly dysoxic–euxinic “(ir)regular” (light pink), and persistently oxic (gray = Sandöfjärden data included; green = Sandöfjärden omitted, see text). For this investigation, we split the sediment cores of Färö Deep and N. Gotland Basin into two segments, reflecting the shift from dysoxic to persistently euxinic conditions over the duration of the sediment deposition covered by our sediment core (Paul et al., 2023a). For all elemental ranges see the Supplementary material (Fig. S3).

combined effect of strongly reducing water column redox conditions and an additional Re input through local anthropogenic activities (i.e., intensive coal combustion, which is the most important energy source in the catchment area), delivered through river discharge and atmospheric deposition (Colodner et al., 1993). In concert with this, Re contents in oxic shelf sediments of the NW Black Sea (St. 13; Lenstra et al., 2019; Paul et al., 2023a) are also unusually high (median:  $\sim 7.36 \mu\text{g kg}^{-1}$  – data not shown – which is  $\sim 2.5$  times the Re contents at German Bight and Sandöfjärden, Fig. 2) given that Re is typically not efficiently sequestered under oxic conditions (Colodner et al., 1993; Nameroff et al., 2002; Chappaz et al., 2008).

The remaining studied elements, i.e., Cd, Cu, Ni, Sb, and Zn, show greater potential as redox proxies, with more clearly distinct content ranges for each redox bin. However, Cd appears to be affected by the shallow SMTZ at Sandöfjärden, similarly to Mo and U (Fig. 5, green vs. gray shaded area), possibly due to efficient uptake into sulfides in the presence of  $\text{H}_2\text{S}$ . Inefficient relative uptake of Cu, Zn, Ni, and Sb into sulfides can be related to complexation with DOM (Section 4.2.2) or association with soluble polysulfides (Wang and Tessier, 2009; Charriau et al., 2011; Herath et al., 2017; Jokinen et al., 2020a), paradoxically making these elements better potential recorders of bottom water redox conditions. Among these metals, Sb stands out by clearly separating oxic and (ir)regularly dysoxic–suboxic sites. Enrichments of Cd, Cu, Zn, and Ni can only reliably separate euxinic from oxic conditions (Fig. 5; Calvert and Pedersen, 1993).

Although many geochemical processes regarding Sb sequestration in coastal (marine) sediments are poorly constrained, recent studies have reported similarities between the behavior of Sb and other elements. Similarly to U, Sb may be sequestered due to redox transformations close to the sediment water interface and be prone to remobilization upon

oxidative dissolution (Chaillou et al., 2008). Similarly to Mo, Sb seems to be affected by Fe and Mn oxide shuttling (Chaillou et al., 2008; Ye et al., 2020; Tribouillard, 2021). The latter could explain elevated Sb contents at Gullmar Fjord (within the range of the more reducing Koljö Fjord and Lilla Värtan), despite a large oxic water column, frequent bottom water reoxidation and low sulfide production rates, limiting the Mo and U sequestration and redox signal preservation in the sediment (Goldberg et al., 2012; Paul et al., 2023b).

Overall, Mo and U remain the most robust (paleo)redox proxies, even in polluted nearshore depositional environments. Although further studies are required to better understand the redox behavior of Sb in coastal systems, our data indicate that additional consideration of Sb can help in separating oxic from dysoxic bottom water when oxic sites with a shallow SMTZ are considered, and in detecting Fe and Mn oxide shuttling. By contrast, we caution against the use of As, V, and Re for reconstruction of redox conditions.

## 5. Conclusions

Our study provides valuable insights into the potentials and limitations of using sedimentary trace metal enrichments as reliable records of environmental and pollution histories in coastal marine environments. The principal outcomes are as follows:

- Our novel approach of summing correlation matrices of site-specific element contents into a single meta-matrix provides a quantitative tool for quickly investigating trace metal correlation patterns as a function of redox or anthropogenic pollution in large data sets.
- A group of predominantly anthropogenically sourced metals (Pb, Cd, Cu, Zn, Sb, Sn, Ni, As, Tl) shows consistently positive inter-element

correlations across a range of study sites, implying a dominant control of the recent input of these metals on sedimentary enrichments.

- A second group of inter-correlated elements with lower anthropogenic impact includes the traditional redox proxies V, Mo, U, Re.
- Sedimentary trace metal contents are generally enhanced under more reducing bottom- and pore water conditions, causing some overlap between the behavior of the two groups of elements. However, redox variability does not necessarily overprint pollution signals. The strongest direct recorders of pollution are Pb and Sn.
- Negative correlations between trace metals and Fe and Mn can help to identify particulate shuttling of trace metals by Fe and Mn oxides.
- The widely observed sedimentary atmospheric 1970s Pb enrichment peak may not be detectable in near-coastal sediments due to the stronger impact of past (legacy) local or regional fluvial Pb point sources, overprinting large-scale atmospheric pollution signals. With increasing distance from shore and local pollution sources, atmospheric Pb pollution signals become more dominant and more reliably to detect in the sediment record.
- We strongly caution against the use of As and V as a redox proxy in coastal settings, while the applicability of Re may be limited by high sedimentation rates and/or low salinities. Further studies are required to verify this.
- Even in polluted depositional environments, redox variability remains the dominant factor in determining sedimentary sequestration of Mo and U.
- When sediments with a shallow SMTZ are overlain by oxic bottom water, Sb shows a greater redox proxy potential than Mo and U, while it can also help detecting Fe and Mn oxide shuttling.

## Funding

This research was funded by the Research Council of Finland (formerly Academy of Finland, grant numbers 1319956 and 1345962), and the Onni Talas Foundation. CPS further acknowledges support by the Dutch Research Council (NWO; Vici-grant number 865.13.005), and the European Research Council (ERC Synergy Marix grant number 854088). This work was carried out under the program of the Netherlands Earth System Science Centre (NESSC), financially supported by the Ministry of Education, Culture and Science (OCW).

## CRedit authorship contribution statement

**K. Mareike Paul:** Writing – original draft, Visualization, Methodology, Investigation, Funding acquisition, Formal analysis, Data curation, Conceptualization. **Niels A.G.M. van Helmond:** Writing – review & editing, Methodology, Investigation, Conceptualization. **Caroline P. Slomp:** Writing – review & editing, Supervision, Methodology, Investigation, Funding acquisition, Conceptualization. **Tom Jilbert:** Writing – review & editing, Supervision, Project administration, Methodology, Funding acquisition, Conceptualization.

## Declaration of competing interest

The authors declare that they have no known competing financial interests or personal relationships that could have appeared to influence the work reported in this paper.

## Data availability

Research data are available from the open access data repository Zenodo (<https://doi.org/10.5281/zenodo.12759164>). Further inquiries can be directed to the corresponding author.

## Acknowledgements

We thank the captain, crew, and scientific participants on board R/V

Skagerrak (2019) and R/V Pelagia (2019) for their assistance with the field work campaigns. We acknowledge the staff of the Kristineberg Marine Research Station and the Royal Netherlands Institute for Sea Research (NIOZ) for their support during the field campaigns. The Geolab, especially Helen de Waard, Coen Mulder, Natasja Welters, and Arnold van Dijk are acknowledged for analytical assistance at Utrecht University. We thank the Hellab technicians, especially Juhani K. Virkanen and Tuija B. Vaahtojärvi are acknowledged for their analytical assistance at the Department of Geosciences and Geography, University of Helsinki. This publication is contribution no. 20 from Hellabs.

## Appendix A. Supplementary data

Supplementary data to this article can be found online at <https://doi.org/10.1016/j.scitotenv.2024.175789>.

## References

- Adelson, J.M., Helz, G.R., Miller, C.V., 2001. Reconstructing the rise of recent coastal anoxia; molybdenum in Chesapeake Bay sediments. *Geochim Cosmochim. Acta* 65, 237–252. [https://doi.org/10.1016/S0016-7037\(00\)00539-1](https://doi.org/10.1016/S0016-7037(00)00539-1).
- Algeo, T.J., Liu, J., 2020. A re-assessment of elemental proxies for paleoredox analysis. *Chem. Geol.* 540 <https://doi.org/10.1016/j.chemgeo.2020.119549>.
- Algeo, T.J., Lyons, T.W., 2006. Mo-total organic carbon covariation in modern anoxic marine environments: implications for analysis of paleoredox and paleohydrographic conditions. *Paleoceanography* 21, PA1016. <https://doi.org/10.1029/2004pa001112>.
- Algeo, T.J., Maynard, J.B., 2004. Trace-element behavior and redox facies in core shales of Upper Pennsylvanian Kansas-type cyclothem. *Chem. Geol.* 206, 289–318. <https://doi.org/10.1016/j.chemgeo.2003.12.009>.
- Algeo, T.J., Tribovillard, N., 2009. Environmental analysis of paleoceanographic systems based on molybdenum–uranium covariation. *Chem. Geol.* 268, 211–225. <https://doi.org/10.1016/j.chemgeo.2009.09.001>.
- Beck, M., Boning, P., Schuckel, U., Stiehl, T., Schnetger, B., Rullkotter, J., et al., 2013. Consistent assessment of trace metal contamination in surface sediments and suspended particulate matter: a case study from the Jade Bay in NW Germany. *Mar. Pollut. Bull.* 70, 100–111. <https://doi.org/10.1016/j.marpolbul.2013.02.017>.
- Bennett, W.W., Canfield, D.E., 2020. Redox-sensitive trace metals as paleoredox proxies: a review and analysis of data from modern sediments. *Earth Sci. Rev.* 204, 103175. <https://doi.org/10.1016/j.earscirev.2020.103175>.
- Billon, G., Ouddane, B., Laureyns, J., Boughriet, A., 2001. Chemistry of metal sulfides in anoxic sediments. *Phys. Chem. Chem. Phys.* 3, 3586–3592. <https://doi.org/10.1039/b102404n>.
- Böning, P., Shaw, T., Pahnke, K., Brumsack, H.J., 2015. Nickel as indicator of fresh organic matter in upwelling sediments. *Geochim Cosmochim. Acta* 162, 99–108. <https://doi.org/10.1016/j.gca.2015.04.027>.
- Böning, P., Ehlert, C., Niggemann, J., Schnetger, B., Pahnke, K., 2017. Thallium dynamics in the Weser estuary (NW Germany). *Estuar Coast Shelf S.* 187, 146–151. <https://doi.org/10.1016/j.ecss.2016.12.004>.
- Borg, H., Jonsson, P., 1996. Large-scale metal distribution in Baltic Sea sediments. *Mar. Pollut. Bull.* 32, 8–21. [https://doi.org/10.1016/0025-326x\(95\)00103-T](https://doi.org/10.1016/0025-326x(95)00103-T).
- Boxberg, F., Asendorf, S., Bartholomae, A., Schnetger, B., de Lange, W.P., Hebbeln, D., 2020. Historical anthropogenic heavy metal input to the south-eastern North Sea. *Geo-Mar. Lett.* 40, 135–148. <https://doi.org/10.1007/s00367-019-00592-0>.
- Boyle, E.A., Edmond, J.M., Sholkovitz, E.R., 1977. The mechanism of iron removal in estuaries. *Geochim Cosmochim. Acta* 41, 1313–1324. [https://doi.org/10.1016/0016-7037\(77\)90075-8](https://doi.org/10.1016/0016-7037(77)90075-8).
- Brännvall, M.L., Bindler, R., Renberg, I., Emteryd, O., Bartnicki, J., Billstrom, K., 1999. The Medieval metal industry was the cradle of modern large scale atmospheric lead pollution in northern Europe. *Environ. Sci. Technol.* 33, 4391–4395. <https://doi.org/10.1021/es990279n>.
- Brännvall, M.L., Bindler, R., Emteryd, O., Renberg, I., 2001. Four thousand years of atmospheric lead pollution in northern Europe: a summary from Swedish lake sediments. *J. Paleolimnol.* 25, 421–435. <https://doi.org/10.1023/A:1011186100081>.
- Brinkmann, I., Barras, C., Jilbert, T., Paul, K.M., Somogyi, A., Ni, S., et al., 2023. Benthic foraminiferal Mn/Ca as low-oxygen proxy in fjord sediments. *Global Biogeochem. Cy.* 37, e2023GB007690 <https://doi.org/10.1029/2023GB007690>.
- Broman, D., Lundbergh, I., Naf, C., 1994. Spatial and seasonal-variation of major and trace-elements in settling particulate matter in an estuarine-like archipelago area in the northern Baltic proper. *Environ. Pollut.* 85, 243–257. [https://doi.org/10.1016/0269-7491\(94\)90045-0](https://doi.org/10.1016/0269-7491(94)90045-0).
- Bruland, K.W., Middag, R., Lohan, M.C., 2014. 8.2 - controls of trace metals in seawater. In: Holland, H.D., Turekian, K.K. (Eds.), *Treatise on Geochemistry*, Second edition. Elsevier, Oxford, pp. 19–51. <https://doi.org/10.1016/B978-0-08-095975-7.00602-1>.
- Bura-Nakić, E., Knezevic, L., Mandić, J., Cindrić, A.M., Omanovic, D., 2021. Rhenium distribution and behavior in the salinity gradient of a highly stratified estuary and pristine riverine waters (the Krka River, Croatia). *Arch. Environ. Contam. Toxicol.* 81, 564–573. <https://doi.org/10.1007/s00244-021-00876-6>.

- Burdige, D.J., 1993. The biogeochemistry of manganese and iron reduction in marine sediments. *Earth Sci. Rev.* 35, 249–284. [https://doi.org/10.1016/0012-8252\(93\)90040-E](https://doi.org/10.1016/0012-8252(93)90040-E).
- Burdige, D.J., 2006. *Geochemistry of Marine Sediments*. Princeton University Press (ISBN-13: 9780691095066).
- Callender, E., 2000. Geochemical effects of rapid sedimentation in aquatic systems: minimal diagenesis and the preservation of historical metal signatures. *J. Paleolimnol.* 23, 243–260. <https://doi.org/10.1023/A:1008114630756>.
- Callender, E., 2014. 11.3 - heavy metals in the environment – historical trends. In: Holland, H.D., Turekian, K.K. (Eds.), *Treatise on Geochemistry*, Second edition. Elsevier, Oxford, pp. 59–89. <https://doi.org/10.1016/B978-0-08-095975-7.00903-7>.
- Calmano, W., Hong, J., Forstner, U., 1993. Binding and mobilization of heavy-metals in contaminated sediments affected by Ph and redox potential. *Water Sci. Technol.* 28, 223–235. <https://doi.org/10.2166/wst.1993.0622>.
- Calvert, S.E., Pedersen, T.F., 1993. Geochemistry of recent oxic and anoxic marine-sediments - implications for the geological record. *Mar. Geol.* 113, 67–88. [https://doi.org/10.1016/0025-3227\(93\)90150-T](https://doi.org/10.1016/0025-3227(93)90150-T).
- Canavan, R.W., Van Cappellen, P., Zwolsman, J.J.G., van den Berg, G.A., Slomp, C.P., 2007. Geochemistry of trace metals in a fresh water sediment: field results and diagenetic modeling. *Sci. Total Environ.* 381, 263–279. <https://doi.org/10.1016/j.scitotenv.2007.04.001>.
- Canfield, D.E., Thamdrup, B., 2009. Towards a consistent classification scheme for geochemical environments, or, why we wish the term ‘suboxic’ would go away. *Geobiology* 7, 385–392. <https://doi.org/10.1111/j.1472-4669.2009.00214.x>.
- Canuto, F.A.B., Garcia, C.A.B., Alves, J.P.H., Passos, E.A., 2013. Mobility and ecological risk assessment of trace metals in polluted estuarine sediments using a sequential extraction scheme. *Environ. Monit. Assess.* 185, 6173–6185. <https://doi.org/10.1007/s10661-012-3015-0>.
- Carignan, R., Tessier, A., Rancourt, L., 2003. Metal deposition chronologies in boreal shield lakes: distinguishing anthropogenic signals from diagenetic effects. *Hum. Ecol. Risk Assess.* 9, 767–777. <https://doi.org/10.1080/713610008>.
- Carpenter, J., Bithell, J., 2000. Bootstrap confidence intervals: when, which, what? A practical guide for medical statisticians. *Stat. Med.* 19, 1141–1164. [https://doi.org/10.1002/\(SICI\)1097-0258\(20000515\)19:9<1141::AID-SIM479>3.0.CO;2-F](https://doi.org/10.1002/(SICI)1097-0258(20000515)19:9<1141::AID-SIM479>3.0.CO;2-F).
- Cato, I., 2006. Miljökvalitet och trender i sediment och biota utmed Bohuskusten 2000/2001 - en rapport från sju kontrollprogram: environmental quality and trends in sediment and biota along the Bohus Coast in 2000/2001 - a report from seven trend-monitoring programmes. 122. Sveriges geologiska undersökning (SGU), Uudevalde. <https://apps.sgu.se/geolagret/GetMetaDataByld?id=md-ec28add7-b864-4cbe-9b04-6d6c61db4e34>.
- Cederqvist, J., Lidstrom, S., Sorlin, S., Svedang, H., 2020. Swedish environmental history of the Baltic Sea a review of current knowledge and perspectives for the future. *Scand. J. Hist.* 45, 663–688. <https://doi.org/10.1080/03468755.2019.1692067>.
- Chaillou, G., Schäfer, J., Blanc, G., Anschutz, P., 2008. Mobility of Mo, U, As, and Sb within modern turbidites. *Mar. Geol.* 254, 171–179. <https://doi.org/10.1016/j.margeo.2008.06.002>.
- Chappaz, A., Gobeil, C., Tessier, A., 2008. Sequestration mechanisms and anthropogenic inputs of rhenium in sediments from eastern Canada lakes. *Geochim Cosmochim. Acta.* 72, 6027–6036. <https://doi.org/10.1016/j.gca.2008.10.003>.
- Charriau, A., Lesven, L., Gao, Y., Leermakers, M., Baeyens, W., Ouddane, B., et al., 2011. Trace metal behaviour in riverine sediments: role of organic matter and sulfides. *Appl. Geochem.* 26, 80–90. <https://doi.org/10.1016/j.apgeochem.2010.11.005>.
- Chow, T.J., Bruland, K.W., Bertine, K., Soutar, A., Koide, M., Goldberg, E.D., 1973. Lead pollution: records in southern California coastal sediments. *Science* 181, 551–552. <https://doi.org/10.1126/science.181.4099.551>.
- Cole, D.B., Zhang, S., Planavsky, N.J., 2017. A new estimate of detrital redox-sensitive metal concentrations and variability in fluxes to marine sediments. *Geochim Cosmochim. Acta.* 215, 337–353. <https://doi.org/10.1016/j.gca.2017.08.004>.
- Colodner, D., Sachs, J., Ravizza, G., Turekian, K., Edmond, J., Boyle, E., 1993. The geochemical cycle of rhenium: a reconnaissance. *Earth Planet Sci Lett.* 117, 205–221. [https://doi.org/10.1016/0012-821x\(93\)90127-u](https://doi.org/10.1016/0012-821x(93)90127-u).
- Colodner, D., Edmond, J., Boyle, E., 1995. Rhenium in the Black-Sea - comparison with molybdenum and uranium. *Earth Planet Sci Lett.* 131, 1–15. [https://doi.org/10.1016/0012-821x\(95\)00010-A](https://doi.org/10.1016/0012-821x(95)00010-A).
- Cooke, C.A., Bindler, R., 2015. Lake sediment records of preindustrial metal pollution. *Dev. Paleoenviron. Res.* 18, 101–119. [https://doi.org/10.1007/978-94-017-9541-8\\_6](https://doi.org/10.1007/978-94-017-9541-8_6).
- Crusius, J., Calvert, S., Pedersen, T., Sage, D., 1996. Rhenium and molybdenum enrichments in sediments as indicators of oxic, suboxic and sulfidic conditions of deposition. *Earth Planet Sci Lett.* 145, 65–78. [https://doi.org/10.1016/S0012-821x\(96\)00204-X](https://doi.org/10.1016/S0012-821x(96)00204-X).
- Dalcin Martins, P., de Monlevad, J.P.R.C., Medrano, M.J.E., Lenstra, W.K., Wallenius, A. J., Hermans, M., et al., 2024. Sulfide toxicity as key control on anaerobic oxidation of methane in eutrophic coastal sediments. *Environ. Sci. Technol.* 58, 11421–11435. <https://doi.org/10.1021/acs.est.3c10418>.
- Dang, D.H., Lenoble, V., Durrieu, G., Omanovic, D., Mullot, J.U., Mounier, S., et al., 2015. Seasonal variations of coastal sedimentary trace metals cycling: insight on the effect of manganese and iron (oxy)hydroxides, sulphide and organic matter. *Mar. Pollut. Bull.* 92, 113–124. <https://doi.org/10.1016/j.marpolbul.2014.12.048>.
- Dijkstra, N., Kraal, P., Séguret, M.J.M., Flores, M.R., Gonzalez, S., Rijkenberg, M.J.A., et al., 2018. Phosphorus dynamics in and below the redoxcline in the Black Sea and implications for phosphorus burial. *Geochim Cosmochim. Acta.* 222, 685–703. <https://doi.org/10.1016/j.gca.2017.11.016>.
- Du Laing, G., Vandecasteele, B., De Grauwe, P., Moors, W., Lesage, E., Meers, E., et al., 2007. Factors affecting metal concentrations in the upper sediment layer of intertidal reedbeds along the river Scheldt. *J. Environ. Monit.* 9, 449–455. <https://doi.org/10.1039/b618772b>.
- Du Laing, G., Rinklebe, J., Vandecasteele, B., Meers, E., Tack, F.M.G., 2009. Trace metal behaviour in estuarine and riverine floodplain soils and sediments: a review. *Sci. Total Environ.* 407, 3972–3985. <https://doi.org/10.1016/j.scitotenv.2008.07.025>.
- EBH-kartan (EBH Map), 2023. Web tool providing information on potentially contaminated areas and contamination risk classes in Sweden (in Swedish). <https://ext-geoportal.lansstyrelsen.se/standard/?appid=ed0d3fde3cc9479f9688c2b2969fd38c> (last access: 12 October 2023).
- Eckert, S., Brumsack, H.J., Severmann, S., Schmetger, B., März, C., Fröhlje, H., 2013. Establishment of euxinic conditions in the Holocene Black Sea. *Geology* 41, 431–434. <https://doi.org/10.1130/G33826.1>.
- EEA, 2019. Contaminants in Europe's Seas - Moving Towards a Clean, Non-toxic Marine Environment. <https://doi.org/10.2800/511375>.
- EEA, 2021. CHASE classification of contaminant status in sediments. <https://www.eea.europa.eu/data-and-maps/figures/chase-classification-of-contaminant-status-1> (last access: February 2023).
- Egger, M., Rasigraf, O., Sapart, C.J., Jilbert, T., Jetten, M.S., Rockmann, T., et al., 2015. Iron-mediated anaerobic oxidation of methane in brackish coastal sediments. *Environ. Sci. Technol.* 49, 277–283. <https://doi.org/10.1021/es503663z>.
- Engqvist, A., Andrejev, O., 2003. Water exchange of the Stockholm archipelago - a cascade framework modelling approach. *J. Sea Res.* 49, 275–294. [https://doi.org/10.1016/S1385-1101\(03\)00023-6](https://doi.org/10.1016/S1385-1101(03)00023-6).
- Farmer, J.G., 1991. The perturbation of historical pollution records in aquatic sediments. *Environ. Geochem. Health* 13, 76–83. <https://doi.org/10.1007/Bf01734298>.
- Filipsson, H.L., Nordberg, K., 2004. Climate variations, an overlooked factor influencing the recent marine environment. An example from Gullmar Fjord, Sweden, illustrated by benthic foraminifera and hydrographic data. *Estuaries* 27, 867–881. <https://doi.org/10.1007/Bf02912048>.
- Förstner, U., Ahlf, W., Calmano, W., Kersten, M., Salomons, W., 1986. Mobility of heavy metals in Dredged Harbor sediments. *Sediments and Water Interactions* 371–380. [https://doi.org/10.1007/978-1-4612-4932-0\\_31](https://doi.org/10.1007/978-1-4612-4932-0_31).
- Förstner, U., Schoer, J., Knauth, H.D., 1990. Metal pollution in the tidal Elbe River. *Sci. Total Environ.* 97–8, 347–368. [https://doi.org/10.1016/0048-9697\(90\)90250-X](https://doi.org/10.1016/0048-9697(90)90250-X).
- Gambrell, R.P., Wiesepape, J.B., Patrick, W.H., Duff, M.C., 1991. The effects of Ph, redox, and salinity on metal release from a contaminated sediment. *Water Air Soil Pollut.* 57–8, 359–367. <https://doi.org/10.1007/Bf00282899>.
- Goldberg, E.D., Hodge, V., Koide, M., Griffin, J., Gamble, E., Bricker, O.P., et al., 1978. A pollution history of Chesapeake Bay. *Geochim Cosmochim. Acta.* 42, 1413–1425. [https://doi.org/10.1016/0016-7037\(78\)90047-9](https://doi.org/10.1016/0016-7037(78)90047-9).
- Goldberg, E.D., Hodge, V.F., Griffin, J.J., Koide, M., Edgington, D.N., 1981. Impact of fossil-fuel combustion on the sediments of Lake-Michigan. *Environ. Sci. Technol.* 15, 466–471. <https://doi.org/10.1021/es00086a013>.
- Goldberg, T., Archer, C., Vance, D., Thamdrup, B., McAnena, A., Poulton, S.W., 2012. Controls on Mo isotope fractionations in a Mn-rich anoxic marine sediment, Gullmar Fjord, Sweden. *Chem. Geol.* 296, 73–82. <https://doi.org/10.1016/j.chemgeo.2011.12.020>.
- Goldschmidt, V.M., 1937. The principles of distribution of chemical elements in minerals and rocks. The seventh Hugo Müller Lecture, delivered before the Chemical Society on March 17th, 1937. *Journal of the Chemical Society (Resumed)* 655–673. <https://doi.org/10.1039/JR9370000655>.
- Guo, T.Z., DeLaune, R.D., Patrick, W.H., 1997. The influence of sediment redox chemistry on chemically active forms of arsenic, cadmium, chromium, and zinc in estuarine sediment. *Environ. Int.* 23, 305–316. [https://doi.org/10.1016/S0160-4120\(97\)00033-0](https://doi.org/10.1016/S0160-4120(97)00033-0).
- Gustafsson, M., Nordberg, K., 1999. Benthic foraminifera and their response to hydrography, periodic hypoxic conditions and primary production in the Koljo fjord on the Swedish west coast. *J. Sea Res.* 41, 163–178. [https://doi.org/10.1016/S1385-1101\(99\)00002-7](https://doi.org/10.1016/S1385-1101(99)00002-7).
- Hallberg, R.O., 1976. A geochemical method for investigation of paleoredox conditions in sediments. *Ambio Special Report* 139–147. <https://www.jstor.org/stable/25099586>.
- Hallberg, R.O., 1991. Environmental implications of metal distribution in Baltic Sea sediments. *Ambio* 20, 309–316. <http://www.jstor.org/stable/4313851>.
- Harland, R., Nordberg, K., Filipsson, H.L., 2006. Dinoflagellate cysts and hydrographical change in Gullmar Fjord, west coast of Sweden. *Sci. Total Environ.* 355, 204–231. <https://doi.org/10.1016/j.scitotenv.2005.02.030>.
- Hebbeln, D., Scheurle, C., Lamy, F., 2003. Depositional history of the Helgoland mud area, German Bight, North Sea. *Geo-Mar. Lett.* 23, 81–90. <https://doi.org/10.1007/s00367-003-0127-0>.
- HELCOM, 2018. State of the Baltic Sea – second HELCOM holistic assessment 2011–2016. In: *Baltic Sea Environment Proceedings*, 155. HELCOM, Helsinki, Finland, pp. 1–155. <https://helcom.fi/baltic-sea-trends/holistic-assessments/state-of-the-baltic-sea-2018/reports-and-materials/>.
- HELCOM, 2021. Inputs of hazardous substances to the Baltic Sea. In: *Baltic Sea Environment Proceedings*, 179. HELCOM Helsinki, Finland, pp. 1–48. <https://helcom.fi/wp-content/uploads/2021/09/Inputs-of-hazardous-substances-to-the-Baltic-Sea.pdf>.
- van Helmond, N.A.G.M., Jilbert, T., Slomp, C.P., 2018. Hypoxia in the Holocene Baltic Sea: comparing modern versus past intervals using sedimentary trace metals. *Chem. Geol.* 473, 478–490. <https://doi.org/10.1016/j.chemgeo.2018.06.028>.
- van Helmond, N.A.G.M., Robertson, E.K., Conley, D.J., Hermans, M., Humborg, C., Kubeneck, L.J., et al., 2020a. Removal of phosphorus and nitrogen in sediments of the eutrophic Stockholm archipelago, Baltic Sea. *Biogeosciences* 17, 2745–2766. <https://doi.org/10.5194/bg-17-2745-2020>.

- van Helmond, N.A.G.M., Loughheed, B.C., Vollebregt, A., Peterse, F., Fontorbe, G., Conley, D.J., et al., 2020b. Recovery from multi-millennial natural coastal hypoxia in the Stockholm Archipelago, Baltic Sea, terminated by modern human activity. *Limnol. Oceanogr.* 65, 3085–3097. <https://doi.org/10.1002/lno.11575>.
- Helz, G.R., 2021. Dissolved molybdenum asymptotes in sulfidic waters. *Geochem. Perspect. Lett.* 19, 23–26. <https://doi.org/10.7185/geochemlet.2129>.
- Helz, G.R., 2022. The Re/Mo redox proxy reconsidered. *Geochim Cosmochim. Ac.* 317, 507–522. <https://doi.org/10.1016/j.gca.2021.10.029>.
- Herath, I., Vithanage, M., Bundschuh, J., 2017. Antimony as a global dilemma: geochemistry, mobility, fate and transport. *Environ. Pollut.* 223, 545–559. <https://doi.org/10.1016/j.envpol.2017.01.057>.
- Huang, Y.S., Freeman, K.H., Wilkin, R.T., Arthur, M.A., Jones, A.D., 2000. Black Sea chemocline oscillations during the Holocene: molecular and isotopic studies of marginal sediments. *Org. Geochem.* 31, 1525–1531. [https://doi.org/10.1016/S0146-6380\(00\)00090-5](https://doi.org/10.1016/S0146-6380(00)00090-5).
- Huerta-Diaz, M.A., Morse, J.W., 1992. Pyritization of trace-metals in anoxic marine-sediments. *Geochim Cosmochim. Ac.* 56, 2681–2702. [https://doi.org/10.1016/0016-7037\(92\)90353-K](https://doi.org/10.1016/0016-7037(92)90353-K).
- Ingrí, J., Widerlund, A., Suteerasak, T., Bauer, S., Elming, S.-Å., 2014. Changes in trace metal sedimentation during freshening of a coastal basin. *Mar. Chem.* 167, 2–12. <https://doi.org/10.1016/j.marchem.2014.06.010>.
- Iron, G., 1994. Schwermetalle in Nordseesedimenten. *Nat. Mus.* 124, 146–159. <https://www.vliz.be/imisdocs/publications/262014.pdf>.
- Jilbert, T., Slomp, C.P., 2013a. Rapid high-amplitude variability in Baltic Sea hypoxia during the Holocene. *Geology* 41, 1183–1186. <https://doi.org/10.1130/g34804.1>.
- Jilbert, T., Slomp, C.P., 2013b. Iron and manganese shuttles control the formation of authigenic phosphorus minerals in the euxinic basins of the Baltic Sea. *Geochim Cosmochim. Ac.* 107, 155–169. <https://doi.org/10.1016/j.gca.2013.01.005>.
- Jilbert, T., Asmala, E., Schröder, C., Tiihonen, R., Myllykangas, J.-P., Virtasalo, J.J., et al., 2018. Impacts of flocculation on the distribution and diagenesis of iron in boreal estuarine sediments. *Biogeosciences* 15, 1243–1271. <https://doi.org/10.5194/bg-15-1243-2018>.
- Jokinen, S.A., Jilbert, T., Tiihonen-Filppula, R., Koho, K., 2020a. Terrestrial organic matter input drives sedimentary trace metal sequestration in a human-impacted boreal estuary. *Sci. Total Environ.* 717, 137047. <https://doi.org/10.1016/j.scitotenv.2020.137047>.
- Jokinen, S.A., Koho, K., Virtasalo, J.J., Jilbert, T., 2020b. Depth and intensity of the sulfate-methane transition zone control sedimentary molybdenum and uranium sequestration in a eutrophic low-salinity setting. *Appl. Geochem.* 122, 104767. <https://doi.org/10.1016/j.apgeochem.2020.104767>.
- Jørgensen, B.B., Bang, M., Blackburn, T.H., 1990. Anaerobic mineralization in marine-sediments from the Baltic-Sea-North-Sea transition. *Mar. Ecol. Prog. Ser.* 59, 39–54. <https://doi.org/10.3354/meps059039>.
- Jørgensen, B.B., Beulig, F., Egger, M., Petro, C., Scholze, C., Roy, H., 2019. Organoclastic sulfate reduction in the sulfate-methane transition of marine sediments. *Geochim Cosmochim. Ac.* 254, 231–245. <https://doi.org/10.1016/j.gca.2019.03.016>.
- Karbassi, A.R., Bassam, S.S., Ardestani, M., 2013. Flocculation of Cu, Mn, Ni, Pb, and Zn during Estuarine Mixing (Caspian Sea). *Int. J. Environ. Res.* 7, 917–924. <https://doi.org/10.22059/ijer.2013.674>.
- Kerner, M., Wallmann, K., 1992. Remobilization events involving Cd and Zn from intertidal flat sediments in the Elbe Estuary during the tidal cycle. *Estuar Coast Shelf S.* 35, 371–393. [https://doi.org/10.1016/S0272-7714\(05\)80034-4](https://doi.org/10.1016/S0272-7714(05)80034-4).
- Kersten, M., Dicke, M., Kriewis, M., Naumann, K., Schmidt, D., Schulz, M., et al., 1988. Distribution and fate of heavy metals in the North Sea. In: Salomons, W., Bayne, B.L., Duursma, E.K., Förstner, U. (Eds.), *Pollution of the North Sea: An Assessment*. Springer Berlin Heidelberg, Berlin, Heidelberg, pp. 300–347. [https://doi.org/10.1007/978-3-642-73709-1\\_19](https://doi.org/10.1007/978-3-642-73709-1_19).
- Kraal, P., Dijkstra, N., Behrends, T., Slomp, C.P., 2017. Phosphorus burial in sediments of the sulfidic deep Black Sea: key roles for adsorption by calcium carbonate and apatite authigenesis. *Geochim Cosmochim. Ac.* 204, 140–158. <https://doi.org/10.1016/j.gca.2017.01.042>.
- Larsen, M.M., Blusztajn, J.S., Andersen, O., Dahlhoff, I., 2012. Lead isotopes in marine surface sediments reveal historical use of leaded fuel. *J. Environ. Monit.* 14, 2893–2901. <https://doi.org/10.1039/c2em30579h>.
- Larsson, A., Lindström, K.N., 2014. Bridging the knowledge-gap between the old and the new: regional marine experience production in Orust, Västra Götaland, Sweden. *Eur. Plan. Stud.* 22, 1551–1568. <https://doi.org/10.1080/09654313.2013.784578>.
- Lee, B.S., Bullister, J.L., Murray, J.W., Sonnerup, R.E., 2002. Anthropogenic chlorofluorocarbons in the Black Sea and the Sea of Marmara. *Deep-Sea Res Pt I.* 49, 895–913. [https://doi.org/10.1016/S0967-0637\(02\)00005-5](https://doi.org/10.1016/S0967-0637(02)00005-5).
- Lehtoranta, J., Bendtsen, J., Lannergren, C., Saarijärvi, E., Lindström, M., Pitkanen, H., 2022. Different responses to artificial ventilation in two stratified coastal basins. *Ecol. Eng.* 179. <https://doi.org/10.1016/j.ecoleng.2022.106611>.
- Lenstra, W.K., Hermans, M., Séguret, M.J.M., Witbaard, R., Behrends, T., Dijkstra, N., et al., 2019. The shelf-to-basin iron shuttle in the Black Sea revisited. *Chem. Geol.* 511, 314–341. <https://doi.org/10.1016/j.chemgeo.2018.10.024>.
- Lenstra, W.K., Séguret, M.J.M., Behrends, T., Groeneveld, R.K., Hermans, M., Witbaard, R., et al., 2020. Controls on the shuttling of manganese over the northwestern Black Sea shelf and its fate in the euxinic deep basin. *Geochim Cosmochim. Ac.* 273, 177–204. <https://doi.org/10.1016/j.gca.2020.01.031>.
- Lenstra, W.K., van Helmond, N.A.G.M., Zygadłowska, O.M., van Zummeren, R., Witbaard, R., Slomp, C.P., 2022. Sediments as a source of iron, manganese, cobalt and nickel to continental shelf waters (Louisiana, Gulf of Mexico). *Front. Mar. Sci.* 9. <https://doi.org/10.3389/fmars.2022.811953>.
- Lenz, C., Jilbert, T., Conley, D.J., Slomp, C.P., 2015. Hypoxia-driven variations in iron and manganese shuttling in the Baltic Sea over the past 8 kyr. *Geochem. Geophys. Geosyst.* 16, 3754–3766. <https://doi.org/10.1002/2015gc005960>.
- Leppäkoski, E., 1968. Some effects of pollution on benthic environment of Gullmarsfjord. *Helgoländer Meeresun.* 17, 291–301. <https://doi.org/10.1007/Bf01611231>.
- Little, S.H., Vance, D., Lyons, T.W., McManus, J., 2015. Controls on trace metal authigenic enrichment in reducing sediments: insights from modern oxygen-deficient settings. *Am. J. Sci.* 315, 77–119. <https://doi.org/10.2475/02.2015.01>.
- Liu, J., Algeo, T.J., 2020. Beyond redox: control of trace-metal enrichment in anoxic marine facies by watermass chemistry and sedimentation rate. *Geochim Cosmochim. Ac.* 287, 296–317. <https://doi.org/10.1016/j.gca.2020.02.037>.
- Luo, M.Y., Zhou, C.Y., Ma, T.H., Guo, W., Percival, L., Baeyens, W., et al., 2022. Anthropogenic activities influence the mobilization of trace metals and oxyanions in coastal sediment porewaters. *Sci. Total Environ.* 839, 156353. <https://doi.org/10.1016/j.scitotenv.2022.156353>.
- Morford, J.L., Emerson, S., 1999. The geochemistry of redox sensitive trace metals in sediments. *Geochim Cosmochim. Ac.* 63, 1735–1750. [https://doi.org/10.1016/S0016-7037\(99\)00126-X](https://doi.org/10.1016/S0016-7037(99)00126-X).
- Morford, J.L., Emerson, S.R., Breckel, E.J., Kim, S.H., 2005. Diagenesis of oxyanions (V, U, Re and Mo) in pore waters and sediments from a continental margin. *Geochim Cosmochim. Ac.* 69, 5021–5032. <https://doi.org/10.1016/j.gca.2005.05.015>.
- Murozumi, M., Chow, T.J., Patterson, C., 1969. Chemical concentrations of pollutant Lead aerosols, terrestrial dusts and sea salts in Greenland and Antarctic snow strata. *Geochim. Cosmochim. Ac.* 33, 1247–1294. [https://doi.org/10.1016/0016-7037\(69\)90045-3](https://doi.org/10.1016/0016-7037(69)90045-3).
- Murray, J.W., Top, Z., Ozsoy, E., 1991. Hydrographic properties and ventilation of the Black-Sea. *Deep-Sea Res.* 38, S663–S689. [https://doi.org/10.1016/S0198-0149\(10\)80003-2](https://doi.org/10.1016/S0198-0149(10)80003-2).
- Nameroff, T.J., Balistrieri, L.S., Murray, J.W., 2002. Suboxic trace metal geochemistry in the eastern tropical North Pacific. *Geochim Cosmochim. Ac.* 66, 1139–1158. [https://doi.org/10.1016/S0016-7037\(01\)00843-2](https://doi.org/10.1016/S0016-7037(01)00843-2).
- Nordberg, K., Gustafsson, M., Krantz, A.L., 2000. Decreasing oxygen concentrations in the Gullmar Fjord, Sweden, as confirmed by benthic foraminifera, and the possible association with NAO. *J. Mar. Syst.* 23, 303–316. [https://doi.org/10.1016/S0924-7963\(99\)00067-6](https://doi.org/10.1016/S0924-7963(99)00067-6).
- Nordberg, K., Filipsson, H.L., Gustafsson, M., Harland, R., Roos, P., 2001. Climate, hydrographic variations and marine benthic hypoxia in Koljö Fjord, Sweden. *J. Sea Res.* 46, 187–200. [https://doi.org/10.1016/S1385-1101\(01\)00084-3](https://doi.org/10.1016/S1385-1101(01)00084-3).
- Nordmyr, L., Åström, M., Peltola, P., 2008a. Metal pollution of estuarine sediments caused by leaching of acid sulphate soils. *Estuar Coast Shelf S.* 76, 141–152. <https://doi.org/10.1016/j.ecss.2007.07.002>.
- Nordmyr, L., Österholm, P., Åström, M., 2008b. Estuarine behaviour of metal loads leached from coastal lowland acid sulphate soils. *Mar. Environ. Res.* 66, 378–393. <https://doi.org/10.1016/j.marenvres.2008.06.001>.
- Norrlin, J., Johansson, H., Larsson, O., Wemming, A., C., N., Rosenqvist, L., et al., 2022. Sedimentundersökningar i svenska kustområden 2021. In: Uppsala, SGU-rapport 2022:16. <https://resource.sgu.se/dokument/publikation/sgurapport/sgurapport202216rapport/s2216-rapport.pdf>.
- Nriagu, J.O., 1989. A global assessment of natural sources of atmospheric trace-metals. *Nature* 338, 47–49. <https://doi.org/10.1038/338047a0>.
- Nriagu, J.O., Pacyna, J.M., 1988. Quantitative assessment of worldwide contamination of air, water and soils by trace-metals. *Nature* 333, 134–139. <https://doi.org/10.1038/333134a0>.
- Olsson, F., 2007. Järnhanterings dynamik: produktion, lokalisering och agglomerationer i Bergslagen och Mellansverige 1368–1910. In: *Umeå Studies in Economic History*, 35. Department of Economic History, Umeå University, 2007, Umeå, p. 210. <https://umu.diva-portal.org/smash/get/diva2:140326/FULLTEXT01.pdf>.
- OSPAR, 2017. Pressures from human activities - contaminants. In: *Intermediate assessment 2017*. OSPAR Commission, London, United Kingdom. <https://oap.ospar.org/en/ospar-assessments/intermediate-assessment-2017/pressures-human-activities/contaminants/>.
- Outridge, P.M., Wang, F.Y., 2015. The stability of metal profiles in freshwater and marine sediments. In: Blais, J., Rosen, M., Smol, J. (Eds.), *Dev. Paleoenv. Res.* 18. Springer, Dordrecht, pp. 35–60. [https://doi.org/10.1007/978-94-017-9541-8\\_3](https://doi.org/10.1007/978-94-017-9541-8_3).
- Pacyna, J.M., Pacyna, E.G., 2001. An assessment of global and regional emissions of trace metals to the atmosphere from anthropogenic sources worldwide. *Environ. Rev.* 9, 269–298. <https://doi.org/10.1139/a01-012>.
- Palanques, A., Diaz, J.L., Farran, M., 1995. Contamination of heavy metals in the suspended and surface sediment of the Gulf of Cadiz (Spain): the role of sources, currents, pathways and sinks. *Oceanol. Acta* 18, 469–477. <https://archimer.ifremer.fr/doc/00097/20791/>.
- Paul, K.M., van Helmond, N.A.G.M., Slomp, C.P., Jokinen, S.A., Virtasalo, J.J., Filipsson, H.L., et al., 2023a. Sedimentary molybdenum and uranium: improving proxies for deoxygenation in coastal depositional environments. *Chem. Geol.* 615, 121203. <https://doi.org/10.1016/j.chemgeo.2022.121203>.
- Paul, K.M., Hermans, M., Jokinen, S.A., Brinkmann, I., Filipsson, H.L., Jilbert, T., 2023b. Revisiting the applicability and constraints of molybdenum- and uranium-based paleo redox proxies: comparing two contrasting sill fjords. *Biogeosciences* 20, 5003–5028. <https://doi.org/10.5194/bg-20-5003-2023>.
- Pham-Gia, T., Hung, T.L., 2001. The mean and median absolute deviations. *Math. Comput. Model.* 34, 921–936. [https://doi.org/10.1016/S0895-7177\(01\)00109-1](https://doi.org/10.1016/S0895-7177(01)00109-1).
- Puls, W., Heinrich, H., Mayer, B., 1997. Suspended particulate matter budget for the German Bight. *Mar. Pollut. Bull.* 34, 398–409. [https://doi.org/10.1016/S0025-3266\(96\)00161-0](https://doi.org/10.1016/S0025-3266(96)00161-0).

- Rasigraf, O., van Helmond, N.A.G.M., Frank, J., Lenstra, W.K., Egger, M., Slomp, C.P., et al., 2020. Microbial community composition and functional potential in Bothnian Sea sediments is linked to Fe and S dynamics and the quality of organic matter. *Limnol. Oceanogr.* 65, S113–S133. <https://doi.org/10.1002/lno.11371>.
- Reimann C, De Caritat P: Chemical Elements in the Environment: Factsheets for the Geochemist and Environmental Scientist, 1, Springer-Verlag Berlin Heidelberg, 1998, IX, 398 pp., ISBN-13: 978-3-642-72016-1.
- Renberg, I., Brännvall, M.L., Bindler, R., Emteryd, O., 2000. Atmospheric lead pollution history during four millennia (2000 BC to 2000 AD) in Sweden. *Ambio* 29, 150–156. [https://doi.org/10.1639/0044-7447\(2000\)029\[0150:Alphdfj\]2.0.Co;2](https://doi.org/10.1639/0044-7447(2000)029[0150:Alphdfj]2.0.Co;2).
- Renberg, I., Bindler, R., Brännvall, M.L., 2001a. Using the historical atmospheric lead-deposition record as a chronological marker in sediment deposits in Europe. *Holocene* 11, 511–516. <https://doi.org/10.1191/095968301680223468>.
- Renberg, I., Bindler, R., Bradshaw, E., Emteryd, O., McGowan, S., 2001b. Sediment evidence of early eutrophication and heavy metal pollution of Lake Mälaren, Central Sweden. *Ambio* 30, 496–502. <https://doi.org/10.1579/0044-7447-30.8.496>.
- Rigaud, S., Radakovitch, O., Couture, R.M., Deflandre, B., Cossa, D., Garnier, C., et al., 2013. Mobility and fluxes of trace elements and nutrients at the sediment-water interface of a lagoon under contrasting water column oxygenation conditions. *Appl. Geochem.* 31, 35–51. <https://doi.org/10.1016/j.apgeochem.2012.12.003>.
- Rooze, J., Egger, M., Tsandev, I., Slomp, C.P., 2016. Iron-dependent anaerobic oxidation of methane in coastal surface sediments: potential controls and impact. *Limnol. Oceanogr.* 61, S267–S282. <https://doi.org/10.1002/lno.10275>.
- Rosenberg, R., 1990. Negative oxygen trends in Swedish coastal bottom waters. *Mar. Pollut. Bull.* 21, 335–339. [https://doi.org/10.1016/0025-326x\(90\)90794-9](https://doi.org/10.1016/0025-326x(90)90794-9).
- Rosenthal, Y., Lam, P., Boyle, E.A., Thomson, J., 1995. Authigenic cadmium enrichments in Suboxic sediments - precipitation and postdepositional mobility. *Earth Planet Sc Lett.* 132, 99–111. [https://doi.org/10.1016/0012-821x\(95\)00056-1](https://doi.org/10.1016/0012-821x(95)00056-1).
- Rowland, J.A., Bland, L.M., James, S., Nicholson, E., 2021. A guide to representing variability and uncertainty in biodiversity indicators. *Conserv. Biol.* 35, 1669–1682. <https://doi.org/10.1111/cobi.13699>.
- Rudnick, R.L., Gao, S., 2014. Composition of the continental crust. *Treatise on Geochemistry* 4, 1–51. <https://doi.org/10.1016/b978-0-08-095975-7.00301-6>.
- Salomons, W., Derooij, N.M., Kerdijk, H., Bril, J., 1987. Sediments as a source for contaminants. *Hydrobiologia* 149, 13–30. <https://doi.org/10.1007/Bf00048643>.
- Schneider, B., Ceburnis, D., Marks, R., Munthe, J., Petersen, G., Sofiev, M., 2000. Atmospheric Pb and Cd input into the Baltic Sea: a new estimate based on measurements. *Mar. Chem.* 71, 297–307. [https://doi.org/10.1016/S0304-4203\(00\)00058-X](https://doi.org/10.1016/S0304-4203(00)00058-X).
- Scholz, F., Neumann, T., 2007. Trace element diagenesis in pyrite-rich sediments of the Achterwasser lagoon, SW Baltic Sea. *Mar. Chem.* 107, 516–532. <https://doi.org/10.1016/j.marchem.2007.08.005>.
- Scholz, F., McManus, J., Sommer, S., 2013. The manganese and iron shuttle in a modern euxinic basin and implications for molybdenum cycling at euxinic ocean margins. *Chem. Geol.* 355, 56–68. <https://doi.org/10.1016/j.chemgeo.2013.07.006>.
- Scholz, F., Baum, M., Siebert, C., Eroglu, S., Dale, A.W., Naumann, M., et al., 2018. Sedimentary molybdenum cycling in the aftermath of seawater inflow to the intermittently euxinic Gotland Deep, Central Baltic Sea. *Chem. Geol.* 491, 27–38. <https://doi.org/10.1016/j.chemgeo.2018.04.031>.
- Scott, C., Lyons, T.W., 2012. Contrasting molybdenum cycling and isotopic properties in euxinic versus non-euxinic sediments and sedimentary rocks: refining the paleoproxies. *Chem. Geol.* 324–325, 19–27. <https://doi.org/10.1016/j.chemgeo.2012.05.012>.
- Sholkovitz, E.R., 1978. The flocculation of dissolved Fe, Mn, Al, Cu, Ni, Co and Cd during estuarine mixing. *Earth Planet Sc Lett.* 41, 77–86. [https://doi.org/10.1016/0012-821X\(78\)90043-2](https://doi.org/10.1016/0012-821X(78)90043-2).
- Shoty, K., Weiss, D., Appleby, P.G., Cheburkin, A.K., Frei, R., Gloor, M., et al., 1998. History of atmospheric lead deposition since 12,370 C yr BP from a peat bog, Jura Mountains, Switzerland. *Science* 281, 1635–1640. <https://doi.org/10.1126/science.281.5383.1635>.
- Slomp, C.P., Malschaert, J.F.P., Lohse, L., VanRaaphorst, W., 1997. Iron and manganese cycling in different sedimentary environments on the North Sea continental margin. *Cont. Shelf Res.* 17, 1083–1117. [https://doi.org/10.1016/S0278-4343\(97\)00005-8](https://doi.org/10.1016/S0278-4343(97)00005-8).
- Slomp, C.P., Mort, H.P., Jilbert, T., Reed, D.C., Gustafsson, B.G., Wolthers, M., 2013. Coupled dynamics of iron and phosphorus in sediments of an oligotrophic Coastal Basin and the impact of anaerobic oxidation of methane. *PLoS One* 8, e62386. <https://doi.org/10.1371/journal.pone.0062386>.
- SMHI (Swedish Meteorological and Hydrological Institute), 2022. Svenskt HavARKivs (SHARK) database: Water chemistry data 1950–2018. <https://sharkweb.smhi.se/havmta-data/> (last access: 03 September 2022).
- Smrzka, D., Zwicker, J., Bach, W., Feng, D., Himmler, T., Chen, D., et al., 2019. The behavior of trace elements in seawater, sedimentary pore water, and their incorporation into carbonate minerals: a review. *Facies* 65, 1–47. <https://doi.org/10.1007/s10347-019-0581-4>.
- Stigebrandt, A., Gustafsson, B.G., 2003. Response of the Baltic Sea to climate change - theory and observations. *J. Sea Res.* 49, 243–256. [https://doi.org/10.1016/S1385-1101\(03\)00021-2](https://doi.org/10.1016/S1385-1101(03)00021-2).
- Stockholms Vattenprogram, 2011. Stockholms Vattenprogram - Årsrapport 2009–2010. Stockholm Vatten, Stockholm, Sweden. [https://miljobarometern.stoekholm.se/content/docs/vp/vattenprogram\\_arsrapport\\_2009-2010.pdf](https://miljobarometern.stoekholm.se/content/docs/vp/vattenprogram_arsrapport_2009-2010.pdf).
- Suess, E., Erlenkeuser, H., 1975. History of metal pollution and carbon input in Baltic Sea sediments. *Meyniana* 27, 63–75. <https://doi.org/10.2312/meyniana.1975.27.63>.
- Sulu-Gambari, F., Roepert, A., Jilbert, T., Hagens, M., Meysman, F.J.R., Slomp, C.P., 2017. Molybdenum dynamics in sediments of a seasonally-hypoxic coastal marine basin. *Chem. Geol.* 466, 627–640. <https://doi.org/10.1016/j.chemgeo.2017.07.015>.
- Theodosi, C., Stavrakakis, S., Koulaki, F., Stavrakaki, I., Moncheva, S., Papathanasiou, E., et al., 2013. The significance of atmospheric inputs of major and trace metals to the Black Sea. *J. Mar. Syst.* 109, 94–102. <https://doi.org/10.1016/j.jmarsys.2012.02.016>.
- Top, Z., Izdar, E., Ergü, M., Konuk, T., 1990. Evidence of Tectonism from <sup>3</sup>He and residence time of helium in the Black Sea. *EOS Trans. Am. Geophys. Union* 71, 1020–1021. <https://doi.org/10.1029/90EO00257>.
- Topcuoglu, S., 2000. Black Sea ecology - pollution research in Turkey of the marine environment. *IAEA Bull.* 42, 12–14. <https://www.iaea.org/publications/magazine/s/bulletin/42-4/black-sea-ecology>.
- Tribouillard, N., 2020. Arsenic in marine sediments: how robust a redox proxy? *Palaeogeogr. Palaeoclimatol. Palaeoecol.* 550, 109745. <https://doi.org/10.1016/j.palaeo.2020.109745>.
- Tribouillard, N., 2021. Conjugated enrichments in arsenic and antimony in marine deposits used as paleoenvironmental proxies: preliminary results. *Bsgf-Earth Sci B.* 192, 39. <https://doi.org/10.1051/bsgf/2021034>.
- Tribouillard, N., Ribouilleau, A., Lyons, T., Baudin, F., 2004. Enhanced trapping of molybdenum by sulfurized marine organic matter of marine origin in Mesozoic limestones and shales. *Chem. Geol.* 213, 385–401. <https://doi.org/10.1016/j.chemgeo.2004.08.011>.
- Tribouillard, N., Algeo, T.J., Lyons, T., Ribouilleau, A., 2006. Trace metals as paleoredox and paleoproductivity proxies: an update. *Chem. Geol.* 232, 12–32. <https://doi.org/10.1016/j.chemgeo.2006.02.012>.
- Valette-Silver, N.J., 1993. The use of sediment cores to reconstruct historical trends in contamination of estuarine and coastal sediments. *Estuaries* 16, 577–588. <https://doi.org/10.2307/1352796>.
- Vallius, H., Alliksaar, T., Suuroja, S., 2022. Changes in heavy metal concentrations in the sediments of the Gulf of Finland over two decades. *Est J Earth Sci.* 71, 177–188. <https://doi.org/10.3176/earth.2022.12>.
- Van der Weijden, C.H., 2002. Pitfalls of normalization of marine geochemical data using a common divisor. *Mar. Geol.* 184, 167–187. [https://doi.org/10.1016/S0025-3227\(01\)00297-3](https://doi.org/10.1016/S0025-3227(01)00297-3).
- Virtasalo, J.J., Osterholm, P., Asmala, E., 2023. Estuarine flocculation dynamics of organic carbon and metals from boreal acid sulfate soils. *Biogeosciences* 20, 2883–2901. <https://doi.org/10.5194/bg-20-2883-2023>.
- Vollebregt, A., van Helmond, N.A.G.M., Pit, S., Kraal, P., Slomp, C.P., 2023. Trace metals as a redox proxy in Arabian Sea sediments in and below the oxygen minimum zone. *Chem. Geol.* 618. <https://doi.org/10.1016/j.chemgeo.2022.121300>.
- Wallenius, A.J., Martins, P.D., Slomp, C.P., Jetten, M.S.M., 2021. Anthropogenic and environmental constraints on the microbial methane cycle in coastal sediments. *Front. Microbiol.* 12, 631621. <https://doi.org/10.3389/fmicb.2021.631621>.
- Wang, F.Y., Tessier, A., 2009. Zero-valent sulfur and metal speciation in sediment porewaters of freshwater lakes. *Environ. Sci. Technol.* 43, 7252–7257. <https://doi.org/10.1021/es8034973>.
- White, W.M., 2018. *Encyclopedia of Geochemistry: A Comprehensive Reference Source on the Chemistry of the Earth*, 1. Springer Cham (ISBN-13: 978-3-319-39312-4).
- Ye, L., Meng, X.G., Jing, C.Y., 2020. Influence of sulfur on the mobility of arsenic and antimony during oxic-anoxic cycles: differences and competition. *Geochim Cosmochim. Acta.* 288, 51–67. <https://doi.org/10.1016/j.gca.2020.08.007>.
- Ytreberg, E., Hansson, K., Hermansson, A.L., Parsmo, R., Lagerström, M., Jalkanen, J.P., et al., 2022. Metal and PAH loads from ships and boats, relative other sources, in the Baltic Sea. *Mar. Pollut. Bull.* 182. <https://doi.org/10.1016/j.marpolbul.2022.113904>.
- Zheng, Y., Anderson, R.F., Van Geen, A., Fleisher, M.Q., 2002. Remobilization of authigenic uranium in marine sediments by bioturbation. *Geochim Cosmochim. Acta.* 66, 1759–1772. [https://doi.org/10.1016/S0016-7037\(01\)00886-9](https://doi.org/10.1016/S0016-7037(01)00886-9).
- Zillén, L., Lenz, C., Jilbert, T., 2012. Stable lead (Pb) isotopes and concentrations - a useful independent dating tool for Baltic Sea sediments. *Quat. Geochronol.* 8, 41–45. <https://doi.org/10.1016/j.quageo.2011.11.001>.